

Distribution Agreement

In presenting this thesis as a partial fulfillment of the requirements for a degree from Emory University, I hereby grant to Emory University and its agents the non-exclusive license to archive, make accessible, and display my thesis in whole or in part in all forms of media, now or hereafter now, including display on the World Wide Web. I understand that I may select some access restrictions as part of the online submission of this thesis. I retain all ownership rights to the copyright of the thesis. I also retain the right to use in future works (such as articles or books) all or part of this thesis.

Min Ji Choi

April 9, 2020

Modification of Quorum Quenching Analogs from *Schinus terebinthifolia* Fruit Extract

by

Min Ji Choi

Dr. Cassandra Quave
Adviser

Department of Chemistry

Dr. Cassandra Quave
Adviser

Dr. Frank McDonald
Committee Member

Dr. Dennis Liotta
Committee Member

2020

Modification of Quorum Quenching Analogs from *Schinus terebinthifolia* Fruit Extract

By

Min Ji Choi

Dr. Cassandra Quave

Adviser

An abstract of
a thesis submitted to the Faculty of Emory College of Arts and Sciences
of Emory University in partial fulfillment
of the requirements of the degree of
Bachelor of Science with Honors

Department of Chemistry

2020

Abstract

Modification of Quorum Quenching Analogs from *Schinus terebinthifolia* Fruit Extract

By Min Ji Choi

With the rise of antibiotic resistance, antivirulence strategies such as quorum quenching have been investigated as an alternative approach to treat bacterial skin infections. From a medicinal plant used to treat wounds in the Brazilian pharmacopeia, *Schinus terebinthifolia* fruit extract “430D-F5” has been reported to attenuate quorum sensing and dermanecrosis in skin infection caused by *Staphylococcus aureus*. With the three bioactive triterpenoids from the extract as precursors, 430F-F5 was modified by ammonolysis, bromination, and epoxidation to investigate the effect on the quorum quenching activity. After monitoring the reaction with high performance liquid chromatography (HPLC), the ammonolyzed products were confirmed by one-dimensional nuclear magnetic resonance (NMR), and the brominated and epoxidated products were detected by liquid chromatography-mass spectrometry (LC-MS). While the ammonolyzed 430F-F5 decreased the quorum quenching activity in accessory gene regulator system (*agr*) I and III of *S. aureus*, the brominated and epoxidated 430F-F5 showed statistically significant increase in the inhibition of *agr* I and III, respectively. However, the fractions of the epoxidated 430F-F5 isolated by the preparative HPLC resulted in a decreased inhibition of *agr* I and III. In this study, semisynthetic quorum quenching analogs generated by ammonolysis, bromination and epoxidation of 430F-F5 were tested on *agr* I and III in *S. aureus* to optimize the antivirulence activity.

Modification of Quorum Quenching Analogs from *Schinus terebinthifolia* Fruit Extract

By

Min Ji Choi

Dr. Cassandra Quave

Adviser

A thesis submitted to the Faculty of Emory College of Arts and Sciences
of Emory University in partial fulfillment
of the requirements of the degree of
Bachelor of Science with Honors

Department of Chemistry

2020

Acknowledgements

I would like to express my gratitude to my advisor, Dr. Cassandra Quave, for making my honors thesis possible with her unwavering mentorship, patience, and belief in my abilities as a researcher. I am grateful for my committee members, Dr. Frank McDonald and Dr. Dennis Liotta, for their insightful advices on designing reactions and characterizing products. I am also thankful for Dr. Fred Strobel for his suggestions in designing and interpreting LC-MS experiments. I would like to acknowledge the staff members and students of the Quave research group: Dr. James Lyles for his extensive knowledge on HPLC and constructive advices on being a successful researcher; Dr. Gina Porras-Brenes for her guidance in designing experiments, interpreting NMR spectra, and proofreading the thesis; Micah Dettweiler for his help with quorum quenching and growth inhibition assays, analysis of bioactivity results, and proofreading the thesis; Monique Salazar for her guidance in using flash chromatography and other lab equipment; Danielle Carrol for her help with the cytotoxicity assay; Marco Caputo for his help with the fraction collector; Dr. Tharanga Samarakoon for providing the voucher of *Schinus terebinthifolia* from the Emory herbarium; Akram Salam, Dr. Huaqiao Tang, Lewis Marquez, and Dr. François Chassagne for their encouragement and support throughout my time at the Quave research group; and the other members for providing a positive and inspirational environment to pursue research. Lastly, my valuable research experience would not have been possible without the love and support from my family, who has always believed in me unconditionally.

Table of Contents

Chapter 1: Introduction	1
Chapter 2: Literature Review	5
Chapter 3: Experimental Procedures	10
Chapter 4: Results and Discussion.....	19
Chapter 5: Conclusion.....	39
References.....	40
Supporting Information.....	44

List of Figures, Schemes, and Tables

Figure 1: Quorum quenching compounds from 430D-F5 of <i>S. terebinthifolia</i> .	4
Scheme 1: Reactions for (a) ammonolysis, (b) bromination 2, and (c) epoxidation 3 of 430F-F5.	4
Figure 2: (a) <i>Schinus terebinthifolia</i> Raddi voucher at Emory University Herbarium, (b) record of <i>S. terebinthifolia</i> in <i>Historia naturalis Brasiliae</i> .	8
Scheme 2: Fractionation of 430F-F5 from <i>S. terebinthifolia</i> fruits with percent yields.	12
Table 1: Solvent used for Bromination 1 and 2.	13
Table 2: Fractionation method for preparative HPLC of epoxidation 3.	16
Figure 3: Analytical HPLC spectra of (a) natural and (b) ammonolyzed 430F-F5 at 254 nm.	19
Figure 4: ¹ H NMR spectra of (a) natural and (b) ammonolyzed 430F-F5 in CDCl ₃ .	20
Figure 5: ¹³ C NMR spectra of (a) natural and (b) ammonolyzed 430F-F5 in CDCl ₃ .	20
Figure 6: Growth inhibition and quorum sensing assays of ammonolyzed 430F-F5.	21
Figure 7: Analytical HPLC spectra of a) bromination 1 and b) bromination 2 at 254 nm.	23
Figure 8: ¹ H NMR spectra of (a) natural and (b) brominated 2 430F-F5 in MeOD.	23
Figure 9: Possible structures of brominated compounds from 430F-F5.	24
Table 3: Chemical formulas and molecular masses of predicted products in Figure 9 .	24
Figure 10: MS spectra of C ₃₀ H ₄₅ O ₃ Br (532.26 m/z) in (a) positive mode at 63.12-64.11 minutes and (b) negative mode at 63.65-64.40 minutes.	25
Figure 11: MS spectra of C ₃₀ H ₄₇ O ₃ Br (534.27 m/z) in (a) positive mode at 64.26-65.20 minutes and (b) negative mode at 52.84-53.79 minutes.	26
Figure 12: Growth inhibition and quorum sensing assays of bromination 2.	27
Figure 13: Analytical HPLC spectra of a) natural 430F-F5, b) epoxidation 1, c) epoxidation 2, and d) epoxidation 3 at 254 nm.	28
Figure 14: ¹ H NMR spectra of (a) natural 430F-F5 and (b) epoxidation 2 in CDCl ₃ .	29
Figure 15: Possible structures of compounds from epoxidated 430F-F5.	30

Table 4: Chemical formula and molecular weight of compounds in Figure 15 .	30
Table 5: Masses of the possible fragments in compound 15e .	30
Figure 16: MS spectra of compound 15e in negative mode for (a) MS, (b) MS 2 on 471 m/z, and (c) MS 3 on 427 m/z at 49.92-50.91 minutes.	31
Figure 17: MS spectra of 15e in negative mode for (a) MS of epoxidated 430F-F5, (b) MS 2 on 471 m/z, and (c) MS 3 on 427 m/z at 54.78-55.37 minutes.	32
Figure 18: Growth inhibition and quorum sensing assays of epoxidation 3.	34
Figure 19: Preparative HPLC spectra of Epoxidation 3 at 217 nm.	34
Figure 20: Growth inhibition and quorum sensing assays of PF 8, 10, 13, 16, 17, 25, 33, and 39 from epoxidation 3.	35
Figure 21: Growth inhibition and quorum sensing assays of PFs from epoxidation 3 at 32 µg/mL.	36
Figure 22: Cytotoxicity assay of natural 430F-F5, bromination 2, and epoxidation 3.	37
Figure 23: ¹ H NMR of a) triterpenoid from natural 430F-F5 and b) epoxidated 430F-F5-PF 27.	38

Chapter 1: Introduction

Quorum Quenching against Antibiotic Resistance

Antibiotic resistance is one of the major health concerns in public health. Serious infections of antibiotic-resistant bacteria affect at least 2 million people in the United States per year and result in at least 23,000 deaths per year.¹ The over prescription and overuse of antibiotics promote the evolution of antibiotic resistance. For example, up to 50% of antibiotic prescriptions are not needed or effective.¹ Because of the emerging antibiotic resistance, the treatment of bacterial infections is challenged by the limited efficiency of antibiotics.²

One way to prevent the passing of genes that contribute to the antibiotic resistance is inhibiting the virulence of bacteria, which prevents the pathogenesis of bacteria that destroys the host. Instead of killing the bacteria, inhibiting the communication among bacteria would decrease the natural selection that pushes the evolution of antibiotic resistance.³ One communication method among bacteria is quorum sensing. As a cell-density dependent mechanism, quorum-sensing regulates the expression of virulence factors like enzymes, hemolysins, and toxins that facilitate the spread of bacteria throughout the tissue. In *Staphylococcus aureus* (MRSA), autoinducing peptide (AIP) is produced and sensed by the four allelic variants of the accessory gene regulator (*agr*) systems.^{4,5} Quenching the *agr* systems inhibits the communication among bacteria and decreases the production of virulence factors.

Natural Products in Drug Discovery

Natural products have influenced the development of new structures for drug discovery. Out of 140 antibacterial drugs approved between 1981 and 2014, 83 drugs were consisted of pure natural products or derived from natural products.⁶ Derived from the fermentation of soil-based

actinobacteria *Dactylosporangium aurantiacum* subspecies *hamdenesis*, Fidaxomicin was approved by the Food and Drug Administration (FDA) in 2011 for the treatment of *Clostridium difficile*-associated diarrhea.⁷

Combinatorial chemistry accelerates drug discovery and development by generating a large number of structurally diverse compounds in a single process.⁸ After the preparation of a combinatorial library, the compounds in the library are screened against a bioactive target, and the bioactive compounds can be identified with bioassay-guided fractionation. Since the scaffolds of natural products are used as lead compounds for various drugs, combinatorial chemistry can be used to transform one library of natural products to another library with modified bioactivity.⁹⁻¹¹

Diversifying plant extracts instead of individual compounds increases the possibility of discovering new bioactive compounds. This approach is efficient when a significant proportion of the mixture is modified. To ensure that the change of the chemical composition in the natural mixture is significant, reactions can target common functional groups in natural products identified by searching common reactive fragments in the CRC Dictionary of Natural Products (DNP version 2001).¹² According to the DNP, the common functional groups found in natural products were the hydroxyl group (75% of the molecules in the database), carbonyl group (73%), double bond (65%), aromatic rings (40%) and nitrogen-containing fragments (23%).¹¹ To discover new scaffolds and increase bioactivity of inactive natural extracts, previous studies have studied reactions that target common functional group found in plant extracts. For example, the reaction between hydrazine monohydrate and a *n*-butanol extract of *Polygonum ferrugineum* Wedd. (Polygonaceae) resulted in products consisting a pyrazole modified from the carbonyl group.¹² The products from the ammonolysis of *P. ferrugineum* increased the antifungal activity

against *Candida albicans*, which was previously not shown in the starting extract. Another common functional groups are the alkene and aromatic rings, which are targeted by bromination. When the natural and brominated extracts of *Conium maculatum* L. (Apiaceae) were tested for the bioactivity against acetylcholinesterase, the brominated extract showed the inhibition of the enzyme.¹⁰ Also, the brominated derivatives from the *Citrus sinensis* L. Osbeck (Rutaceae) peels showed moderate antibacterial activity against *Staphylococcus aureus* but with increased toxicity against mammalian cells.¹³

Project Aims

From investigating traditional medicine used to treat infections and wounds, the Quave group has discovered that “430D-F5” extract from *Schinus terebinthifolia* Raddi (Anacardiaceae) fruits shows an *agr*-quenching activity in methicillin-resistant *Staphylococcus aureus* (MRSA).⁴ The bioassay-guided fractionation of 430D-F5 resulted in three bioactive triterpenoids (**Figure 1**).¹⁴ In this study, quorum-quenching analogs were generated by modifying the functional groups in 430F-F5 of *S. terebinthifolia* fruits. Based on the structures of the bioactive compounds from 430D-F5, different reactions were tested on the extract to modify functional groups such as ketone, alkene, and carboxylic acid (**Scheme 1**). After characterizing the modified extracts with analytical HPLC, NMR, and LC-MS, the modified extracts were tested for the inhibition of *agr* I and III in *S. aureus* and compared with the bioactivity of the natural extract. The modified extract with the improved quorum quenching activity was separated using the preparative HPLC, and the bioactivity of the resulting fractions were assessed with growth inhibition and quorum sensing assays.

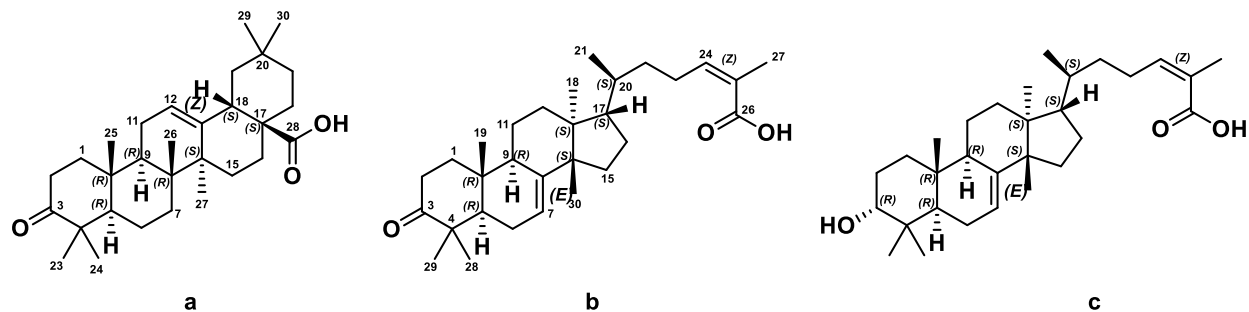
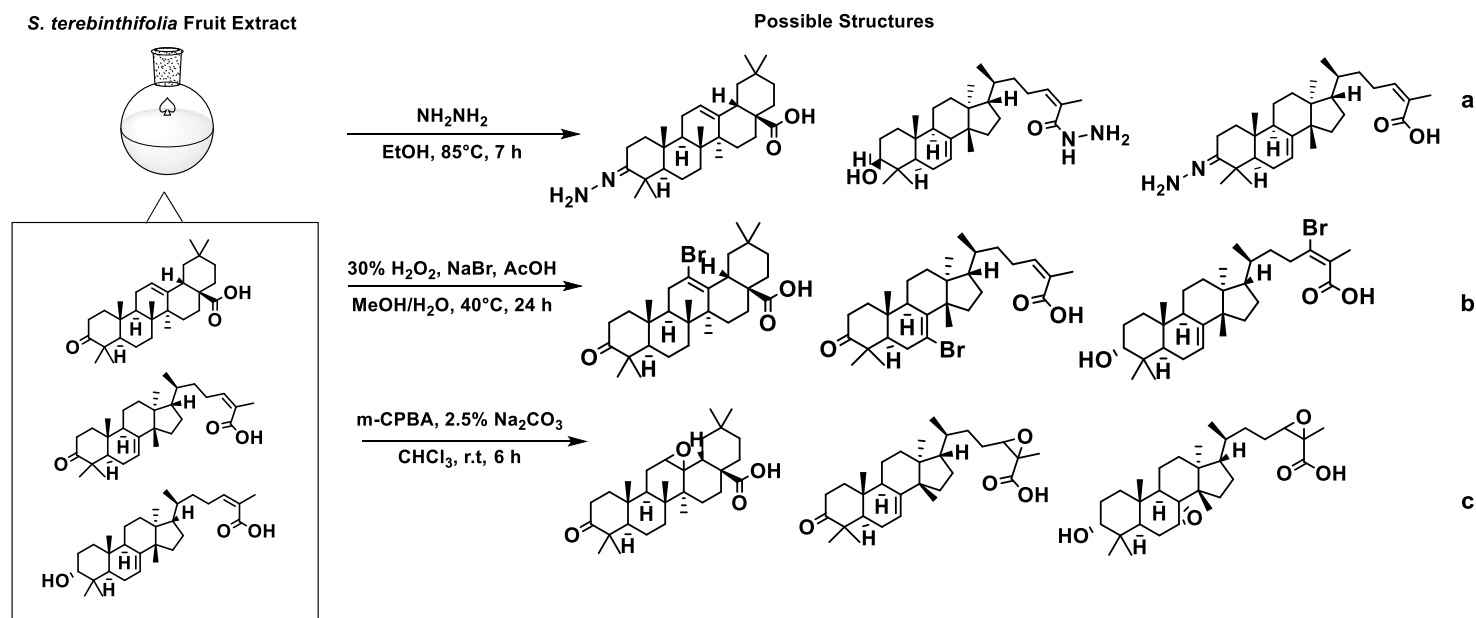


Figure 1: Quorum quenching compounds from 430D-F5 of *S. terebinthifolia*.¹⁴



Scheme 1: Reactions for (a) ammonolysis, (b) bromination 2 (see **Figure 8** for all possible products from bromination), and (c) epoxidation 3 of 430F-F5 (see **Figure 13** for all possible products from epoxidation).

Chapter 2: Literature Review

Common Mechanisms of Antibiotics

The mechanisms of antibiotics include inhibition of cell wall synthesis, protein synthesis and nucleic acid replication and repair mechanisms.³ β lactams and cephalosporins inhibit the transpeptidation of the peptidoglycan, which blocks the biosynthesis of the cell wall. While the macrolides inhibit the exit tunnel of the larger 50S subunit, the tetracyclines target the A-site of aminoacyl-tRNA for the smaller 30s subunit. Another class of quinolones binds to the cleavage sites to prevent the DNA topoisomerase II from cutting the DNA strands for underwinding. However, bacteria have evolved to resist the antibiotic mechanisms by several methods.³ First, the efflux pumps act as active transporters to pump out antibiotics from the bacterial cell. The bacteria can also evolve to mutate or modify binding sites, which prevent the binding of antibiotics on the target. The drug metabolism in bacterial cells can degrade the bioactivity of antibiotics by chemically modifying the structures of the antibiotics.

Antivirulence as Alternative Approach to Antibiotic Resistance

Examples of antibiotics that inhibit the synthesis of cell wall are penicillin and methicillin.¹⁵ After the emergence of penicillin and methicillin-resistant strains, vancomycin is now used to treat MRSA infection.¹⁵ As the vancomycin-resistant strain is also on the rise, antivirulence drugs are now developed to target virulence factors instead of the vital growth mechanism of bacteria. Not only antivirulence drugs decrease the evolutionary pressure for antibiotic resistance, but antivirulence also does not significantly affect the commensal flora of the host.¹⁶ Since most commensal bacteria do not produce toxins, the beneficial bacteria would not be targeted by antivirulence agents. Antivirulence drugs have been developed to inhibit different virulence factors of *S. aureus*. For example, the monoclonal antibody (MAb) 2A3

against alpha toxin (AT) attenuates the inflammation and damage associated with *S. aureus* pneumonia.¹⁷ Triazolothiadiazoles decreases the mortality rate of *S. aureus* sepsis in mice by inhibiting sortase A (SrtA enzyme), which anchors immune evasion proteins to the cell wall.¹⁸

Virulence Factors of *Staphylococcus aureus*

Virulence factors secreted by *Staphylococcus aureus* cause severe disease pathogenesis through skins, tissues, and bloodstream.¹⁷ When transmitted through bloodstream, the virulence factors produced by *S. aureus* can cause metastatic infection, septic shock, and toxin-mediated diseases such as toxic-shock syndrome (TSS) and scalded-skin syndrome (SSS).^{19, 20} The use of highly absorbent tampons can cause menstrual TSS, in which the staphylococcal superantigens toxins transmitted into blood circulation through the cervix or vagina may lead to multiple organ failures.²⁰ When the body is infected by the exfoliative toxins of *S. aureus*, SSS causes rashes and skin peeling mainly in children. *S. aureus* can also lead to pneumonia by secreting the AT.¹⁷

The pathogenesis of *S. aureus* depends on the expression of virulence factors regulated by the accessory gene regulator (*agr*) system.²¹ In *S. aureus*, the four types of *agr* alleles (*agr* I, II, III, IV) respond to corresponding AIP signals (AIP I, II, III, and IV). Each *agr* allele is associated with a staphylococcal disease. While *agr* I is predominant in methicillin-resistant strains, *agr* III is responsible for regulating accessory gene products that cause TSS. Exfoliatin-producing strains that cause SSS belong to *agr* IV. *agr* I is prevalent in community-associated genotypes,¹⁵ and *agr* II is mainly associated to healthcare-associated MRSA strains and biofilm formation.^{22, 23}

Ethnopharmacological Approach to Drug Discovery

Ethnopharmacology is the study of the traditional use of plants for medicine, and plants from pharmacopeias have been investigated for drug discovery. One example of traditional medicine as a lead in drug discovery is artemisinin, an antimalarial drug extracted from *Artemisia annua* L.²⁴ The use of *A. annua* to treat malaria symptoms was discovered in the traditional Chinese medicine. After the extraction of artemisinin based on the description in Ge Hong's *A Handbook of Prescriptions for Emergencies*, the derivatives of artemisinin were successfully developed to treat malaria caused by *Plasmodium falciparum*.²⁴

Schinus terebinthifolia Raddi (Anacardiaceae), commonly known as the Brazilian pepper tree, is a shrub-like tree used in the Brazilian traditional medicine (**Figure 2a**).²⁵ While *S. terebinthifolia* is native to South America, it was introduced in the southeastern United States as an invasive species, particularly in Florida.²⁶ As a part of the Brazilian pharmacopoeia, *S. terebinthifolia* has been used as to treat wounds, ulcers, and urinary and respiratory infections,²⁷ which was recorded in *Historia naturalis Brasiliae* (**Figure 2b**).²⁸ Each parts of *S. terebinthifolia* are prepared using different methods to treat illnesses (see Figure 1c from Muhs et al., 2017).⁴

Bioactivity of Triterpenoids

S. terebinthifolia is consisted of phenolic derivatives such as gallic acid, methyl gallate, tannins, flavonoids, and terpenes.²⁷ Known for its fragrance in essential oil, terpenes are second metabolites that attract pollinators and repel predators.³³ Categorized by the number of five-carbon isoprene units, triterpenes are consisted of six isoprene units.²⁹ Triterpenoids extracted from the butanol extract of *S. terebinthifolia* fruits inhibited quorum sensing in *Staphylococcus aureus*.⁴ Triterpenoids extracted from other plants show different bioactivity. Triterpene acids from frankincense inhibited microsomal prostaglandin E2 synthase (mPGES-1) as an anti-inflammatory compounds.³⁴ Derived from Cucurbitaceae and Cruciferae, cucurbitacin D showed anti-cancer activity in doxorubicin-resistant breast cancer cells.³⁵

Lead Optimization in Drug Discovery

After natural products are identified as lead compounds for bioactivity, the structures of the lead compounds are modified to improve the potency and selectivity.³⁶ Methods to optimize the properties of lead compounds include improving lipophilicity and adding polar groups to improve absorption and oral bioavailability. Since nonalkylating epoxides are less likely to react with nucleophiles, stable epoxides are added to improve the solubility and metabolic stability by modifying pKa.³⁷ However, unstable epoxides can be hepatotoxic or carcinogenic by alkylating proteins or nucleic acid in the liver. In other case, alkenes transformed to epoxides can shorten the half-life of a drug due to its metabolism to 1,2-diols. While halogenated bonds can also be toxic, halogenated bonds can improve the thermal and oxidative stability and membrane permeability of a compound and decrease its probability of oxidation by liver P450 detoxification enzymes.¹³

Chapter 3: Experimental Procedures

Collection of Plant Material

In November 2013 and 2014, the leaves, stems, and fruits of *Schinus terebinthifolia* Raddi were collected from private lands in DeSoto County, Florida with the permission of the landowner. The collection and identification of bulk and voucher specimens followed the procedures from 2003 World Health Organization (WHO) Guidelines for good agricultural and collection practices (GACP) for medicinal plants. Populations with possible exposure to herbicides were excluded. Deposited at the Emory University Herbarium (GEO) (Voucher CQ-400, GEO Accession No. 020063), the vouchers were identified by using the standard Flora for Florida.³⁸ After the leaves, stems, and fruits of the plant were manually separated and cleansed of contaminants, the plant materials was dried in a drying cabinet at low heat. The plant material was then stored in paper bags at room temperature.

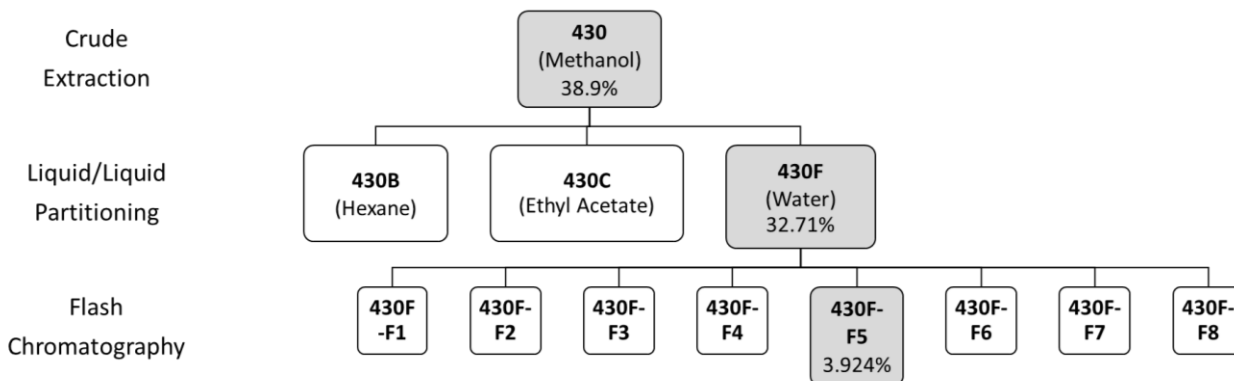
General Experimental Procedures

The NMR spectroscopic data of the natural and modified extracts in CDCl₃ and CD₃OD were acquired with Bruker 400 and Bruker AVANCE III HD 600 (600 MHz for ¹H-NMR, 5 mm CryoProbe) spectrometers. Chemical shifts are in parts per million, and the NMR spectra were processed with MNOVA and TopSpin. Analytical high-performance liquid chromatography (HPLC) were performed with Thermo Scientific LTQ-FT Ultra MS equipped with a Shimadzu SIL-ACHT and Dionex 3600SD HPLC pump. The LC-FTMS spectra were obtained using a Thermo Scientific LTQ-FT Ultra MS equipped with a Shimadzu SIL-ACHT and Dionex 3600SB HPLC pump with Eclipse XDB-C18 5 μm 4.6 x 250 mm at room temperature. LC-MS spectra were processed and analyzed by Thermo-Fischer's Xcalibur.

Sodium bromide (99%, ACS reagent), sodium bicarbonate (99.7%, ACS reagent) were obtained from Sigma-Aldrich. m-CPBA (77% max) was obtained from Aldrich. Sodium carbonate decahydrate (99+% for analysis) and hydrazine monohydrate was purchased from Acros-organic. Anhydrous potassium carbonate was purchased from Fischer bioreagents. Sodium sulfate (ACS), methanol, hexane, CH₂Cl₂, ethyl acetate, ethanol, and acetonitrile were purchased from VWR chemicals. Glacial acetic acid and sodium hydroxide pellets were obtained from Macrons fine chemicals. Hydrogen peroxide (30%) was obtained from Electron Microscopy Sciences.

Extraction of 430F from *Schinus terebinthifolia*

The dried *Schinus terebinthifolia* fruits were blended in methanol with a ratio of 1 g plant material to 10 mL MeOH using a Waring commercial blender for 5 minutes. The material was filtered after sonicating for 20 minutes. The sonication and decantation were repeated in total of three times. The combined filtered extracts were evaporated using a rotary evaporator at temperature less than 40 °C and lyophilized. The dried extracts were dissolved in 20% MeOH (aq) at 1 g:33 mL and separated by liquid-liquid partitioning three times with an equal volume of hexane, EtOAc, and H₂O saturated n-butanol. After drying the organic layers over Na₂SO₄ and filtered, the organic layers were further dried under reduced pressure. The organic and aqueous layers from the partition with H₂O saturated n-butanol was labeled as 430D and 430E, which were combined to give 430F (**Scheme 2**).



Scheme 2: Fractionation of 430F-F5 from *S. terebinthifolia* fruits with percent yields.

Fractionation of 430F by Flash Chromatography

430F was fractionated using a CombiFlash Rf+ Lumen (Teledyne ISCO) flash chromatography system with a RediSep Rf Gold silica column and three solvent system of (A) hexane, (B) DCM, and (C) MeOH. 430F was binded to Celite 545 with a ratio of 1:4 as a dry load column. The gradient started with 100% A for 6 column volumes (CV), changed to 100% B over 12 CV. After holding the gradient at 100% B for 18.2 CV, the gradient switched to 74.5:25.5 B:C over 3.1 CV and held for 6.8 CV. The gradient changed to 68.8:31.2 B:C over 0.7 CV, followed by a hold for 7.5 CV. Finally, the gradient went to 100% C over 2.2 CV and held for 14.6 CV. The chromatography was detected by evaporative light scanning detector (ELSD) at 254 and 280 nm. The fractionation resulted in 8 fractions: 430F-F1 (tubes 1-0), 430F-F2 (11-17), 430F-F3 (18-27), 430F-F4 (28-43), 430F-F5 (44), 430F-F6 (45-62), 430F-F7 (63-71), and 430F-F8 (72-79).

Ammonolysis

Hydrazine monohydrate (500 uL) was added to 430F-F5 (400 mg) in ethanol (25 mL). The reaction mixture was stirred for 8 hours at 80 °C. The reaction mixture was evaporated and diluted with water (50 mL). The aqueous phase was extracted with dichloromethane (50 mL x 3). The organic phases were dried with sodium sulfate and evaporated. Caution must be taken when handling hydrazine monohydrate to avoid the combustion and toxicity from the vapors of hydrazine monohydrate.³⁹

Bromination

NaBr (455 mg) in acetic acid (20 mL) and 30% H₂O₂ (220 uL) were added to 430F-F5 (200 mg) in the solvent system according to **Table 1** (30 mL). The reaction mixture was stirred for 24 hours at 40 °C. The solvent was evaporated, and the reaction mixture was diluted with water (60 mL). The organic phase was extracted with ethyl acetate (60 mL x 3). The combined organic phases were dried with sodium sulfate and evaporated. Bromination 1 and 2 were tested with different solvent system due to the solubility of *S. terebinthifolia* extract (**Table 1**). As precautionary measures, excess H₂O₂ can be destroyed with MnO₂ or Na₂SO₃ and checked for the absence of the peroxide activity by spotting the aqueous solution on starch-potassium iodide impregnated paper before evaporating the solvent.⁴⁰ The use of H₂O₂ with acetone as solvent should be avoided.

Table 1: Solvent used for Bromination 1 and 2.

Reaction	Solvent Ratio
Bromination 1	DI water:MeCN:MeOH = 2:2:1
Bromination 2	DI water:MeOH = 1:1

Epoxidation

Epoxidation 1: 30% H₂O₂ (2 mL) and 4M aqueous NaOH solution (1 mL) were added to the solution of 430F-F5 (300 mg) dissolved in CH₂Cl₂/MeOH (60 mL and 120 mL, 1:2). After the reaction mixture was stirred at room temperature for 45 minutes, DI water (150 mL) was added to quench the reaction. The organic layer was extracted with CH₂Cl₂ (200 mL x 3). The combined organic phases were dried with sodium sulfate and evaporated.

Epoxidation 2 and 3: m-Chloroperoxybenzoic acid (77% max, 150 mg) and 2.5% sodium carbonate (7 mL) were added to 430F-F5 (200 mg) in chloroform (25 mL). The reaction mixture was stirred for 3 hours and 6 hours at room temperature for epoxidation 2 and 3, respectively. The reaction mixture was diluted with dichloromethane (25 mL) and saturated sodium bicarbonate solution (50 mL). The organic phase was extracted with dichloromethane (50 mL x 2). The combined organic phase was washed with saturated sodium bicarbonate (100 mL x 2) and water (100 mL x 2). The organic phase was dried with sodium sulfate and evaporated. The same precautions of H₂O₂ (see experimental procedure for bromination) apply for reducing peroxides from m-CPBA before evaporating the solvent.⁴¹

Analytical HPLC Characterization of Modified Extracts

The modified extracts were characterized by HPLC using Eclipse XDB-C18 5 μ m 4.6 x 250 mm at 40 °C. The samples were dissolved in HPLC grade methanol at the concentration of 10 mg/mL with the injection volume of 10 μ L. The HPLC run was a gradient of 0.1% formic acid in water (A) and 0.1% formic acid in acetonitrile (B) at 1.9 mL/min. The mobile phase was 80:20 A:B at 0 min, 70:30 A:B at 10 min, 60:40 A:B at 25 min, and ending with a column flush at 98:2 A:B at 45 min for 15 min.

Characterization of Brominated and Epoxidated 430F-F5 by LC-FTMS

The sample preparation and chromatography gradient were carried out as previously described. The mobile phase was 70:30 A:B at 0 min held for 3 minutes, 30:70 A:B at 18 min and held for 25 minutes, 25:75 A:B at 45.5 min and held for 12.5 minutes, 0:100 A:B at 63 min held for 15 minutes, ending with, 30:70 A:B at 78.1 min held for 10 minutes. With the scan of 150-1500 m/z , the spectra were obtained in negative and positive electrospray ionization mode (ESI) and processed with Thermo Scientific Xcalibur 2.2 SP1.48 (San Jose, CA).

Solvent Gradient Development for Preparative HPLC of Epoxidation 3

The analytical HPLC was modified to meet the capacity of the preparative HPLC and improve the resolution of the peaks. The analytical HPLC chromatograms was obtained using Eclipse XDB-C18 5 μm 4.6 x 250 mm at 23 °C. The HPLC run was a gradient of 0.1% formic acid in water (A) and 0.1% formic acid in acetonitrile (B) at 1.0 mL/min. The mobile phase was 70:30 A:B at 0 min, 30:70 A:B at 15 min and held for 25 minutes, 25:75 A:B at 42.5 min and held for 12.5 minutes, and ending with 0:100 A:B at 60 min held for 15 minutes. The preparative HPLC was scaled up using Eclipse XDB-C18 5 μm 30 x 250 mm at room temperature and the flow rate of 42.50 mL/min with 2.50 min added to each gradient point. The fractionation method was developed based on the HPLC chromatogram of epoxidation 3 and collected using a LEGO MINDSTORMS fraction collector (**Table 2**).⁴²

Table 2: Fractionation method for preparative HPLC of epoxidation 3.

Fractions	Retention Time (min)				
		13	19-20	27	46
1	1-2	14	21-22	28	47-48
2	3	15	23-24	29	49-51
3	4	16	25	30	52-55
4	5	17	26-28	31	56-59
5	6	18	29-30	32	60-61
6	7-8	19	31	33	62-63
7	9	20	32	34	64
8	10	21	33-34	35	65
9	11-14	22	35	36	66
10	15	23	37-37	37	67
11	16-17	24	38-39	38	68
12	18	25	40-42	39	69-70
		26	43-45	40	71-75

Growth Conditions of *Staphylococcus aureus*

Fluorescent reporter strains (*agr* I and III) of *Staphylococcus aureus* were maintained on tryptic soy agar (TSA), and liquid cultures were prepared in tryptic soy broth (TSB) with constant shaking at 230 rpm overnight. Chloramphenicol (10 µg/mL) was added to all media for these strains to maintain mutant plasmids.

Growth Inhibition Assay

Assays were tested according to Clinical & Laboratory Standards Institute (CLSI) M100-S23 guidelines.⁴³ To prepare the working culture, the liquid culture was standardized with a BioTek Cytation 3 and inoculated into CAHMB to a concentration of 5×10^5 CFU. The working culture was added to the samples of natural and modified 430F-F5 in a 96-well microtiter plates (Grenier-Bio 655-185) with 0.2 mL of total volume for each well. The natural and modified 430F-F5 were serially diluted to produce concentrations of 0.5 to 64 µg/mL. The optical density

was recorded using a BioTek Cytation3 plate reader before and after incubating the plates of *S. aureus* at 37 °C for 18 hours. The growth inhibition was calculated with the following equation:

$$\left(1 - \left(\frac{\Delta OD_{test}}{\Delta OD_{vehicle}}\right)\right) = \% \text{ growth inhibition. Ampicillin was used as a positive control.}$$

Quorum Quenching Assay

Microbroth dilutions with *agr* I and III reporter strains and sub-MIC concentrations of natural and modified 430F-F5 were set up as in the growth inhibition assay using black 96-well plates (Corning, New York). The plates were incubated at 37 °C with constant shaking at 1200 rpm in a humidified chamber. Fluorescence (493 nm excitation, 535 nm emission) and optical density (OD) (600 nm) were measured at 0 and 18 hours. Inhibition of quorum sensing was

calculated with the following formula: $\left(1 - \left(\frac{\Delta RFU_{test}}{\Delta RFU_{vehicle}}\right)\right) = \% \text{ fluorescence.}$

Cytotoxicity Assay

The cytotoxicity of the extracts were examined by using human immortalized keratinocytes (HaCaT) and a lactate dehydrogenase (LDH) cytotoxicity assay (G-Biosciences, St. Louis, MO) as previously described.⁴⁴ Briefly, the cell culture was standardized to 4×10^4 cells/mL using a hemocytometer and 0.2 mL added per well in a tissue culture treated 96-well microtiter plate (Falcon 35–3075). The plates were incubated for 48 hours to allow seeding prior to the exposure of fresh media with treatment. The extracts were serially diluted 2-fold (4–512 µg/mL) and were processed 24 hours later following manufacturer’s protocol for chemical induced cytotoxicity.

Statistical Testing

The multiple t-test grouped analysis by GraphPad Prism 7 software (GraphPad Software, La Jolla, CA) was used to determine the statistical significance of the data. DMSO was used as a vehicle control and compared to the experimental samples with three replicates. $P < 0.05$ was considered as statistically significant.

Chapter 4: Results and Discussion

Ammonolysis, bromination and epoxidation of 430F-F5 were monitored using the analytical HPLC, and the end products were analyzed by using NMR and LC-MS of natural and modified 430F-F5. After confirming the efficiency of the reactions, the reaction mixtures from ammonolysis, bromination 2, and epoxidation 3 were tested for growth inhibition and quorum quenching against *agr* I and *agr* III of *S. aureus*.

Ammonolysis

Hydrazine monohydrate replaces ketone, esters, or carboxylic acid with hydrazones or acyl hydrazides.¹² The ketone and carboxylic acid groups of 430F-F5 was modified by reacting 430F-F5 with hydrazine monohydrate for 8 hours. The change in the chemical composition of 430F-F5 was confirmed by the appearance of new peaks at 254 nm in the analytical HPLC chromatogram of the ammonolyzed extract (**Figure 3**).

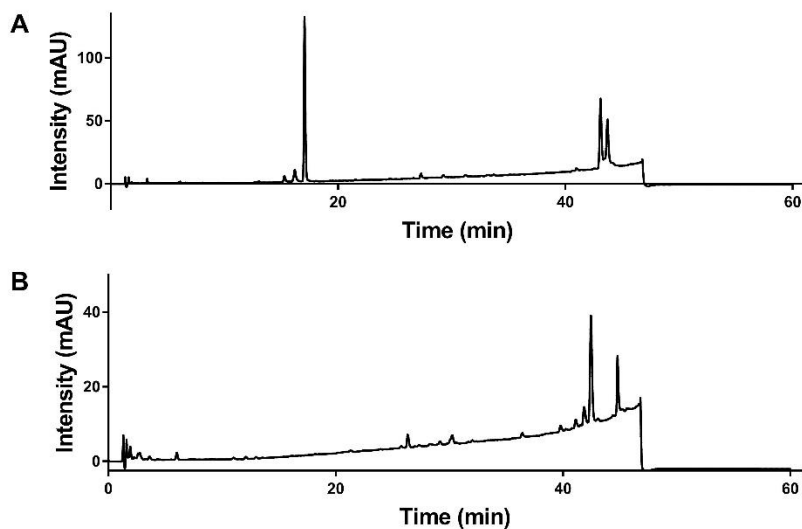


Figure 3: Analytical HPLC chromatograms of (a) natural and (b) ammonolyzed 430F-F5 at 254 nm.

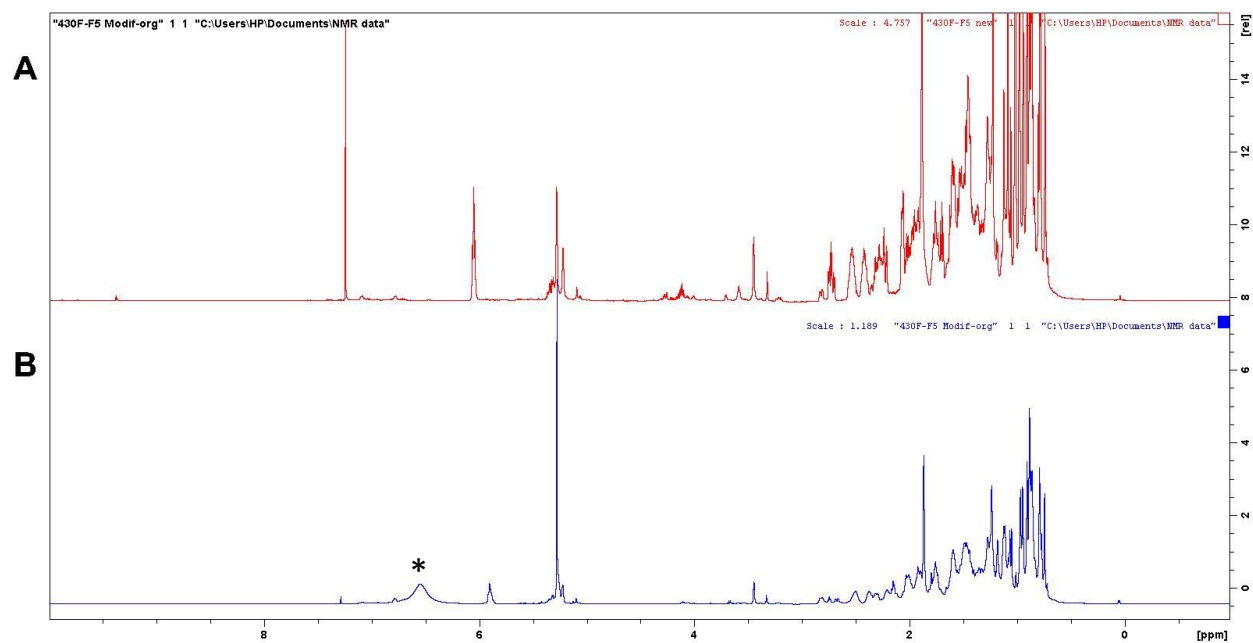


Figure 4: ^1H NMR spectra of (a) natural and (b) ammonolyzed 430F-F5 in CDCl_3 .

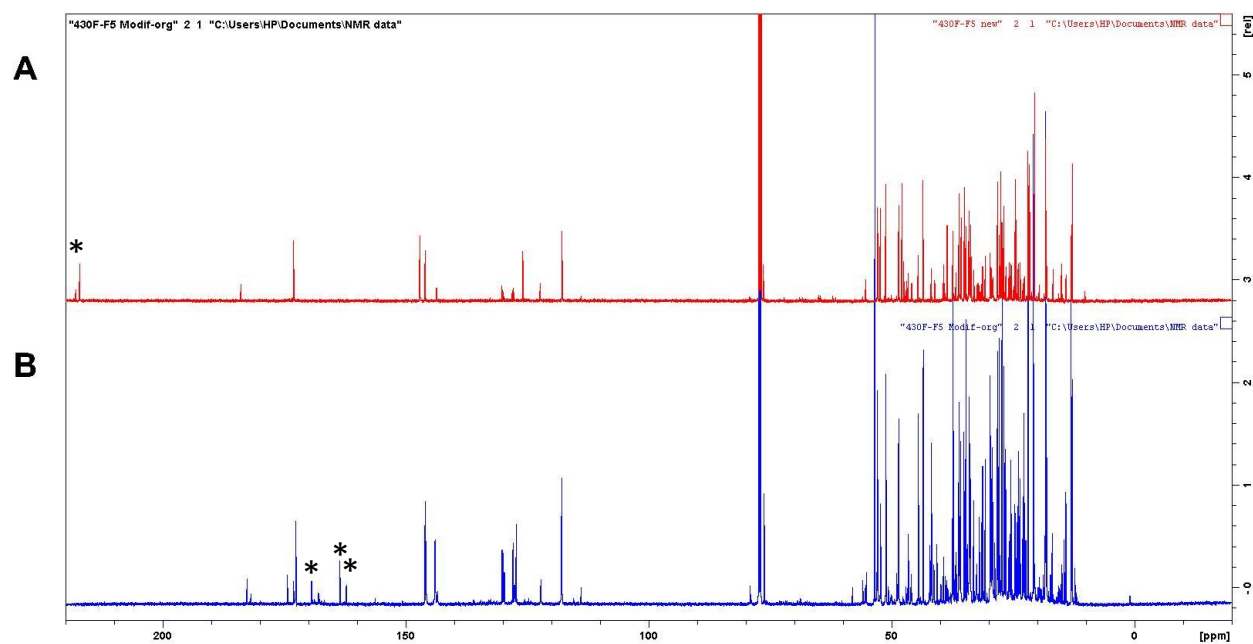


Figure 5: ^{13}C NMR spectra of (a) natural and (b) ammonolyzed 430F-F5 in CDCl_3 .

After the reaction, the proton and carbon NMR spectra and HPLC chromatograms of natural and modified extracts were compared. The reaction was predicted to result in the disappearance of the signals for carbonyl carbons of ketones, esters, aldehydes at 160 and 210 ppm and appearance of the signals for carbons of hydrazine and acyl hydrazides at 150-175 ppm.¹² The formation of hydrazine and acyl hydrazides is indicated by the appearance of a peak around 6.50 ppm in the proton NMR spectrum and 160-180 ppm in the carbon NMR spectrum of the modified extract (**Figures 4 and 5**). The disappearance of a peak around 217 ppm in the carbon NMR spectrum of the natural extract indicated the replacement of carbonyl group with hydrazones and hydrazines (**Figure 5**).

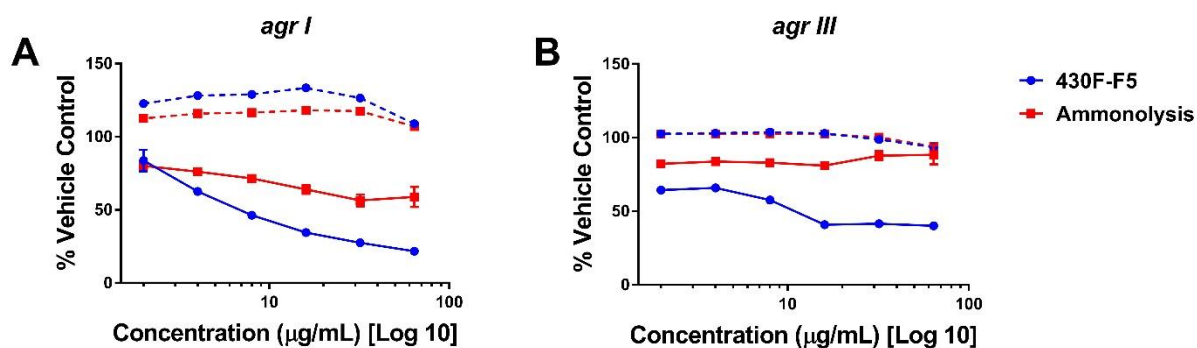


Figure 6: Ammonolyzed 430F-F5 decreased the inhibition of quorum sensing in (a) *agr I* and (b) *agr III*. The solid lines represent the *agr* activity measured by fluorescence, and the dashed lines represent the growth of *S. aureus* measured by optical density.

After confirming the ammonolysis of 430F-F5 using NMR, the ammonolyzed 430F-F5 was tested for the inhibition of quorum sensing in *agr I* and *III* and growth of *S. aureus*. Since the purpose of the study is to optimize the antivirulence activity, the inhibition of quorum sensing should increase without affecting the bacterial growth. While the growth inhibition did not drop below 100% vehicle control, the ammonolyzed 430F-F5 decreased the inhibition of

quorum sensing for both *agr* I and III (**Figure 6**). The modification of the substituent at carbon 3 of compounds **1a-c** does not inhibit the bacterial growth but may play a significant role in the inhibition of virulence factors.

Bromination

430F-F5 was also reacted with hydrogen peroxide and sodium bromide for 24 hours to substitute the alkenyl hydrogen with bromine. The solvent system of the bromination method by Righi *et al.* had to be optimized due to the solubility of the *S. terebinthifolia* extract.¹³ The first bromination was tested with a solution of methanol, water, and acetonitrile. Due to the insolubility of 430F-F5 in acetonitrile, a solution of methanol and water was used for the second bromination.

Compared to the chromatogram of the natural extract, the chromatograms of the first and second brominations showed new peaks between 20 and 45 minutes at 254 nm, which confirmed the change of chemical composition (**Figure 7**). The HPLC chromatograms and NMR spectra of first and second bromination were similar, which indicated that changing the solvent system did not affect the efficiency of the reaction significantly (**Figure 7 and 8**).

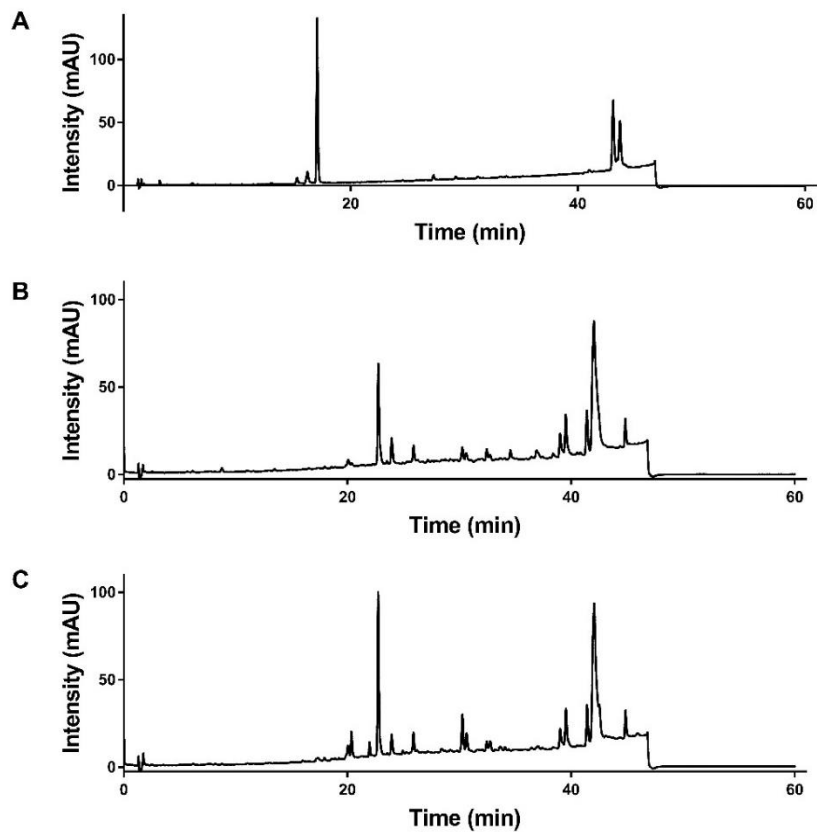


Figure 7: Analytical HPLC chromatograms of a) bromination 1 and b) bromination 2 at 254 nm.

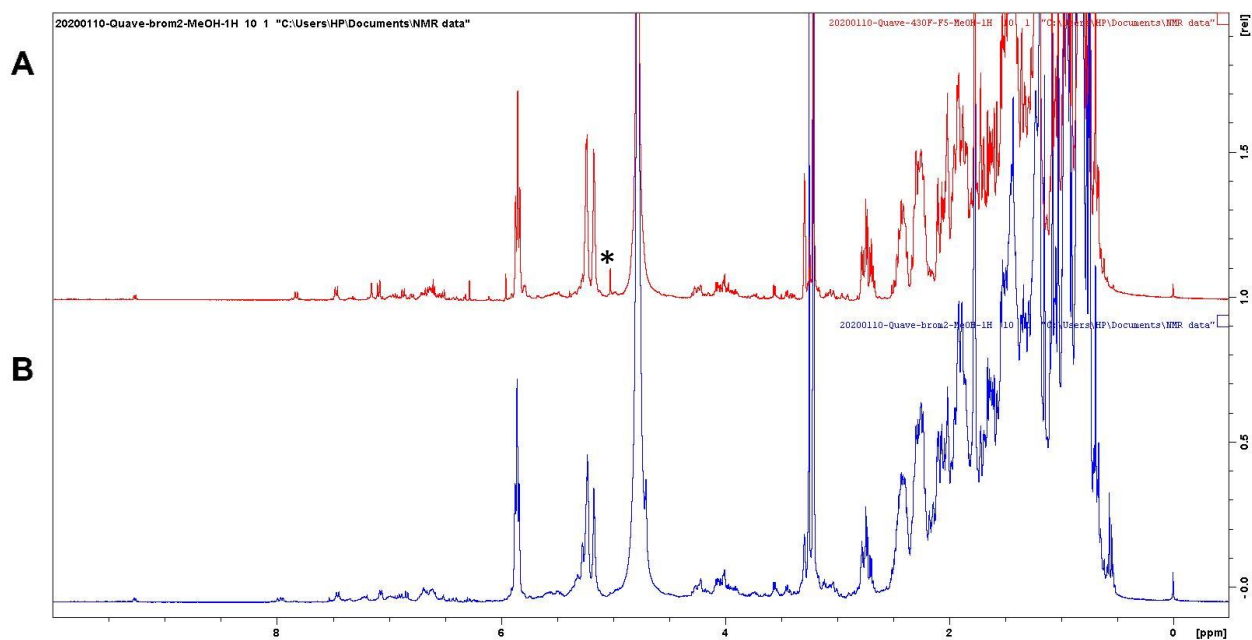


Figure 8: ¹H NMR spectra of (a) natural and (b) brominated 2 430F-F5 in MeOD.

Since the method is reported to substitute alkenyl and phenyl hydrogens in flavonoids with bromine,^{13, 45} the ¹H NMR spectra of the natural and modified 430F-F5 were compared to check for the disappearance of olefinic hydrogen around 5 ppm. The signals for olefinic hydrogen did not completely disappear in the NMR spectra of bromination 2 (**Figure 8**). It is possible that the bromination method resulted in a mixture of compounds brominated at different olefinic hydrogens, which left other olefinic hydrogen unreacted (**Figure 9**).

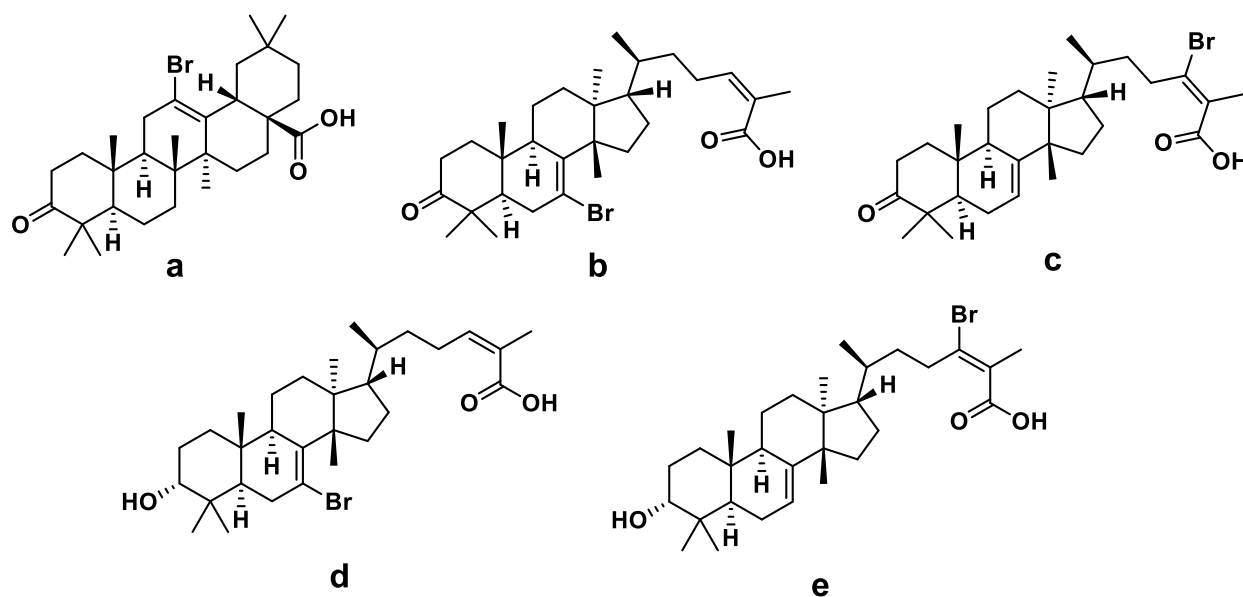


Figure 9: Possible structures of brominated compounds from 430F-F5.

Table 3: Chemical formulas and molecular masses of predicted products in **Figure 9**.

Compound	Chemical Formula	Molecular Mass
9a, 9b, 9c	C ₃₀ H ₄₅ O ₃ Br	532.26
9d, 9e	C ₃₀ H ₄₇ O ₃ Br	534.27

Since the isotopes of bromine, ^{79}Br and ^{81}Br , have 1:1 ratio of relative abundance, the LCMS spectra of compounds containing one bromine show two peaks separated by 2 m/z with a similar height. To confirm the bromination of compounds from 430F-F5, LC-MS was performed on the second bromination. In the LC-MS spectra of the brominated 430F-F5, the peaks appeared at the masses of the predicted products with the 1:1 isotopic ratio of bromine (**Table 3, Figures 10 and 11**). To determine which hydrogen was substituted by bromine, the compounds can be isolated by preparative HPLC and elucidated using NMR. The 1:2:1 ratio for the presence of two bromines in the precursor compounds was not observed in the LC-MS spectra. Overall, the bromination of the precursor compounds indicated the bromination of 430F-F5.

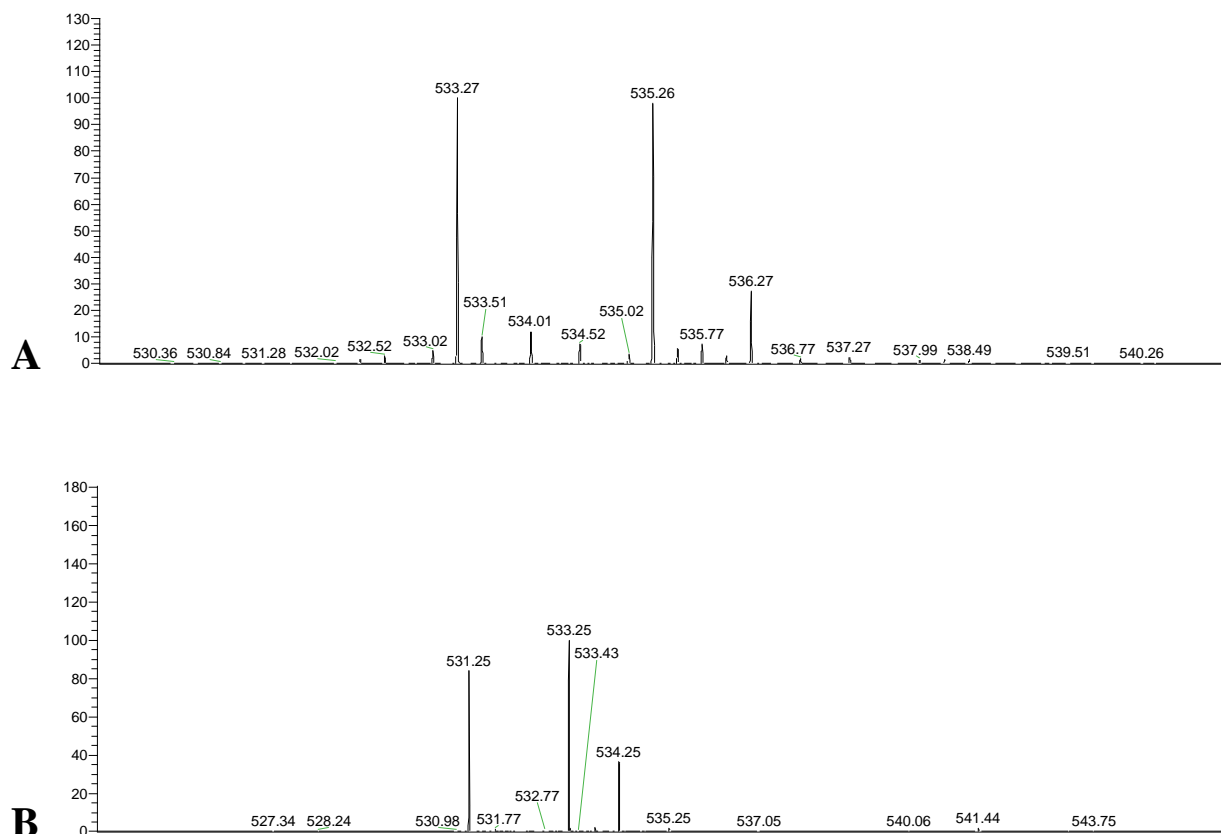


Figure 10: MS spectra of $\text{C}_{30}\text{H}_{45}\text{O}_3\text{Br}$ (532.26 m/z) in (a) positive mode at 63.12-64.11 minutes and (b) negative mode at 63.65-64.40 minutes (see full spectra on **Figure S2**).

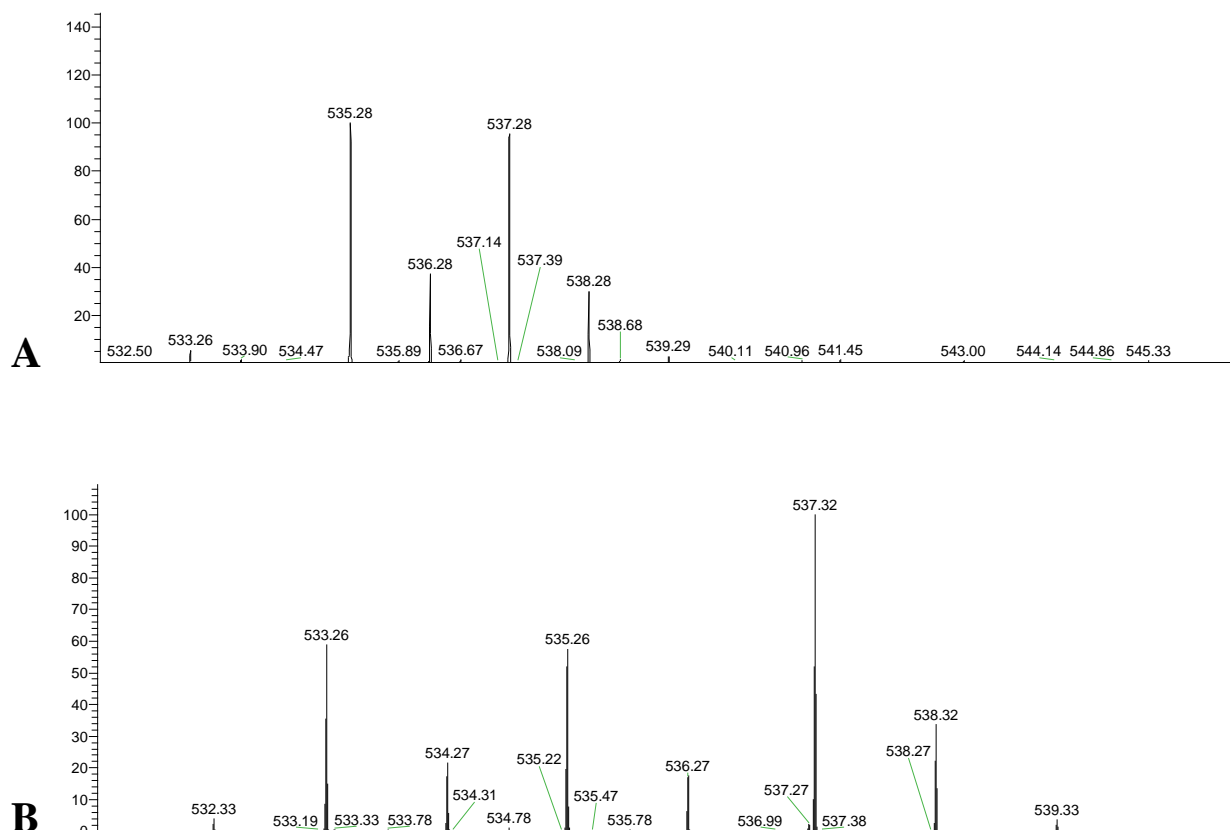


Figure 11: MS spectra of C₃₀H₄₇O₃Br (534.27 m/z) in (a) positive mode at 64.26-65.20 minutes and (b) negative mode at 52.84-53.79 minutes (see full spectra on **Figure S3**).

After the bromination of 430F-F5, the quorum sensing and growth inhibition assays of bromination 2 were obtained. With little or no inhibition of bacterial growth, brominated 430F-F5 showed slight improvement in quorum quenching for *agr* I and no change in inhibition of *agr* III (**Figure 12**). The half maximal inhibitory concentration (IC₅₀) were 8 and 16 µg/mL against *agr* I and III, respectively. The little or no change in the quorum sensing activity was observed in the brominated 430F-F5, because the substitution of the alkenyl proton with bromine did not modify the stereochemistry of the triterpenoid skeleton nor the substituents of carbon 3 of the triterpenoids.

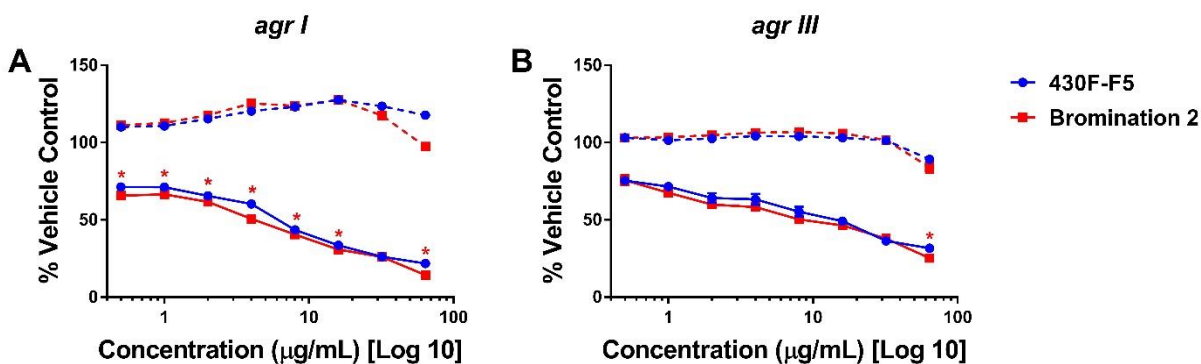


Figure 12: The brominated extract shows slight improvement in inhibition of (a) *agr I* and no significant change at most concentrations on (b) *agr III*. The solid lines represent the *agr* activity measured by fluorescence, and the dashed lines represent the growth of *S. aureus* measured by optical density. The asterisk (*) indicates a significant difference between natural and brominated 430F-F5 with P value less than 0.05 by multiple t-test grouped analysis.

Epoxidation

430F-F5 was reacted with H_2O_2 and NaOH for the first epoxidation following a previously reported method by Llanos *et al.*⁴⁶ The chromatogram of the first epoxidation with hydrogen peroxide only consisted of two peaks (**Figure 13b**), which questioned the inefficiency of the reaction. The peak at 4.75-5.0 ppm in the ^1H NMR spectrum of epoxidation 1 may indicate the proton from R-OH due to the degradation of hydrogen peroxide used in the reaction (**Figure S4**).

To ensure the formation of epoxides, the second epoxidation was tested using a different epoxidation method with meta-chloroperoxybenzoic acid (m-CPBA).⁴⁷ The same method was used for the third epoxidation with the doubled reaction time for a complete epoxidation. The second and third epoxidation led to approximately 10 new peaks with similar retention time and different intensities in the chromatograms (**Figure 13c and 13d**).

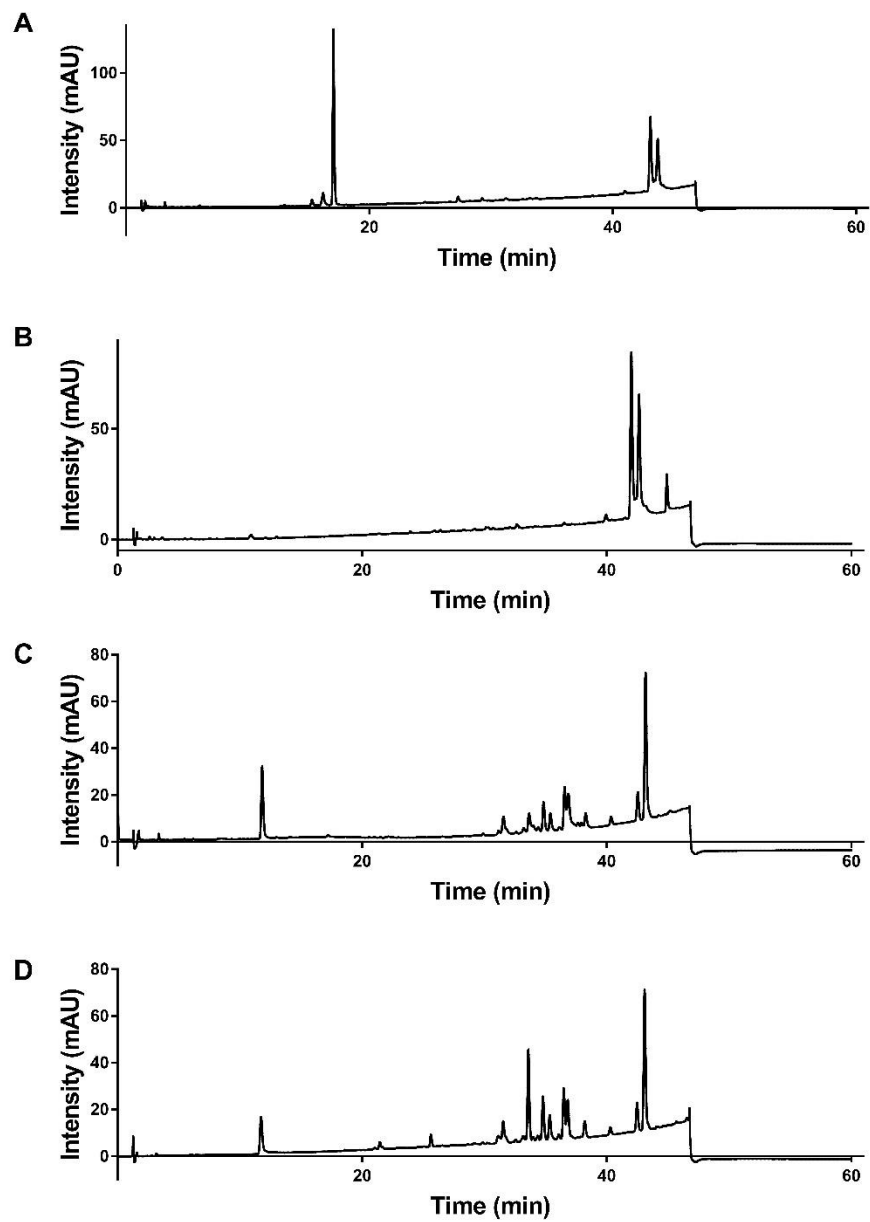


Figure 13: Analytical HPLC chromatograms of a) natural 430F-F5, b) epoxidation 1, c) epoxidation 2, and d) epoxidation 3 at 254 nm.

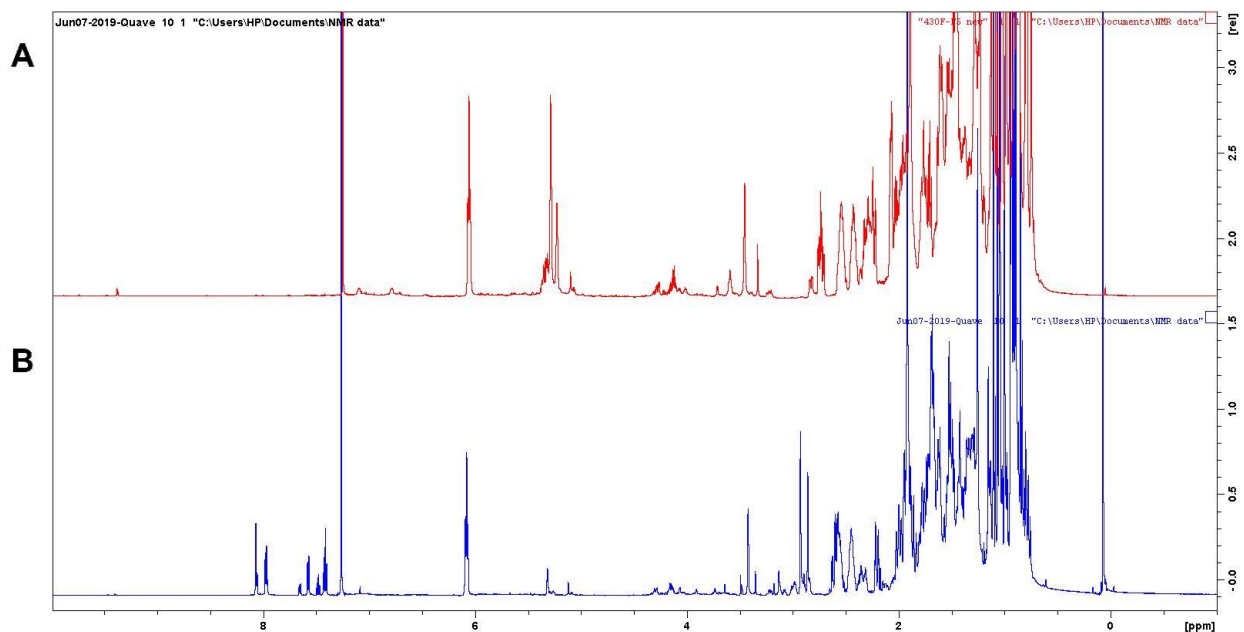


Figure 14: ^1H NMR spectra of (a) natural 430F-F5 and (b) epoxidation 2 in CDCl_3 .

Since m-CPBA reacts with alkenes to form epoxides, proton NMR spectra was obtained to check for the presence of alkenes around 5 ppm. No changes in NMR spectra of epoxidation 2 and 3 were observed, which indicates that the prolonged reaction time does not form more epoxides (**Figure 14**, see **Figure S4** for spectrum of epoxidation 3). In the proton NMR spectra of epoxidation 2 and 3, the intensity of the peaks at 5.0-5.5 ppm decreased (**Figure 14**). While the decreased intensity of the peaks indicates that some alkenes reacted to form epoxides, the peaks at 5.0-5.5 ppm did not completely disappear. Some compounds in 430F-F5 (**Figure 1**) are consisted of more than one alkene, and the reaction may result in a mixture of epoxides reacted with different alkenes (**Figure 15**). The peaks between 7 and 8 ppm are likely the signals of the byproducts m-CPBA or meta-chlorobenzoic acid (**Figure 14**).⁴⁸

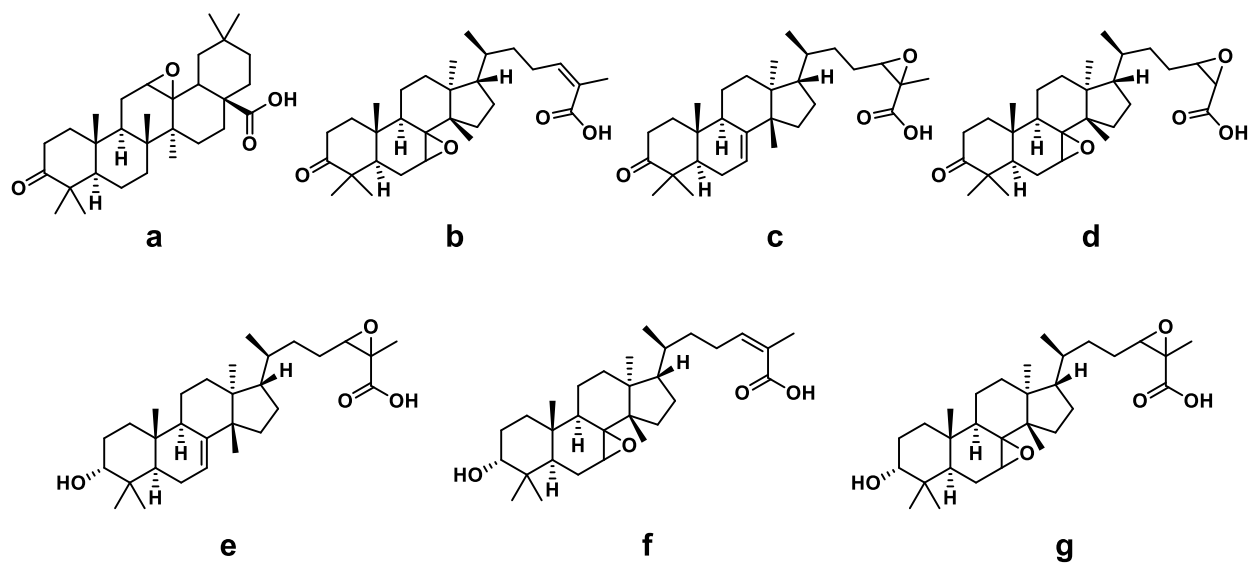


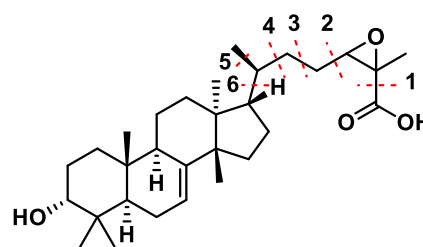
Figure 15: Possible structures of compounds from epoxidated 430F-F5.

Table 4: Chemical formula and molecular weight of compounds in **Figure 15**.

Compound	Chemical Formula	Molecular Mass
15a-c	$C_{30}H_{46}O_4$	470.34
15e, 15f	$C_{30}H_{48}O_4$	472.36
15d	$C_{30}H_{46}O_5$	486.33
15g	$C_{30}H_{48}O_5$	488.35

Table 5: Masses of the possible fragments in compound **15e**.

Fragmentation	Mass
None	472.36
1	427.36
2	371.33
3	357.32
4	343.30
4+5	327.27
6	315.27



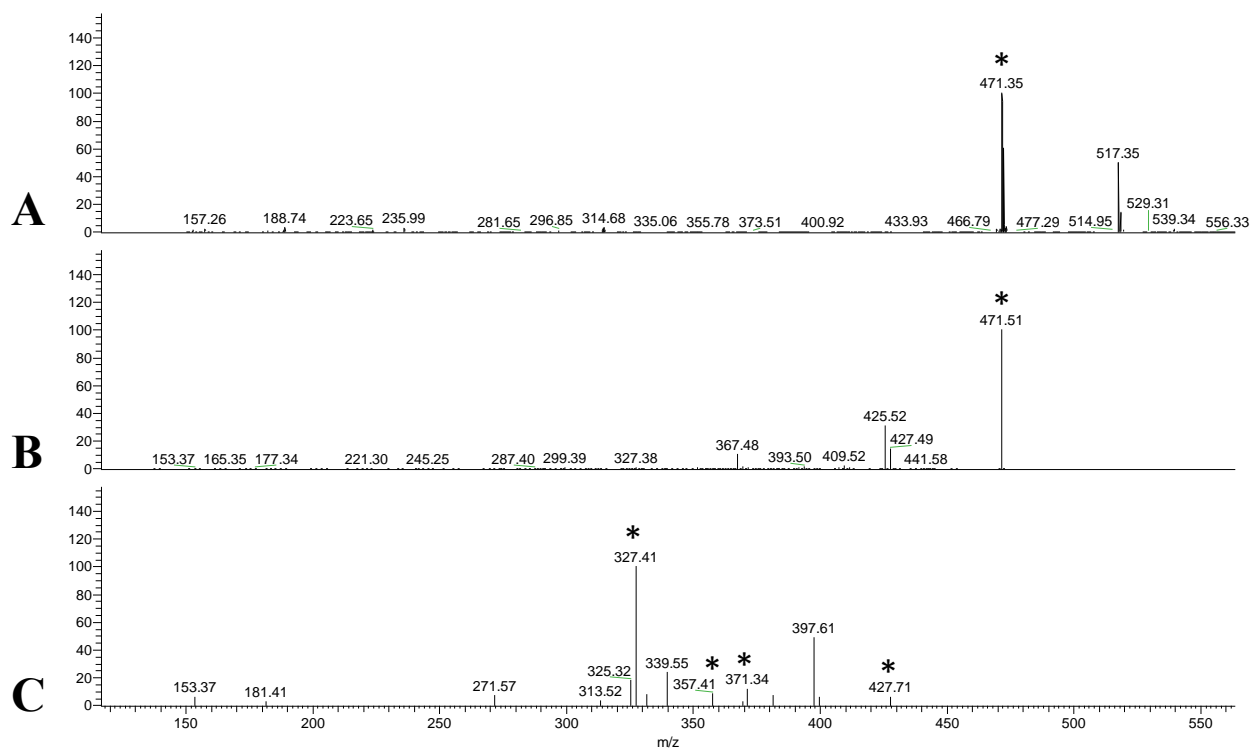


Figure 16: MS spectra of compound **15e** in negative mode for (a) MS, (b) MS 2 on 471 m/z, and (c) MS 3 on 427 m/z at 49.92-50.91 minutes (see full spectra in **Figure S6**). The peaks of the predicted fragments are indicated with an asterisk.

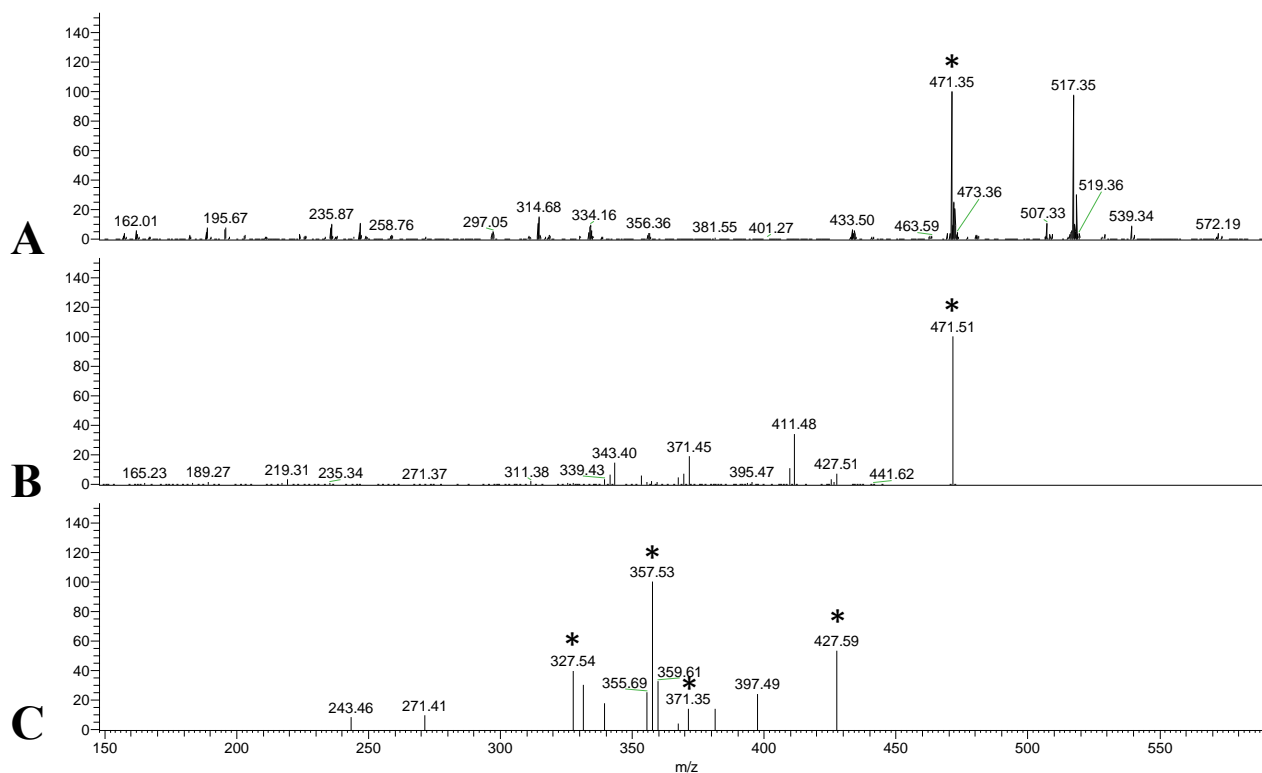


Figure 17: MS spectra of **15e** in negative mode for (a) MS of epoxidated 430F-F5, (b) MS 2 on 471 m/z, and (c) MS 3 on 427 m/z at 54.78-55.37 minutes (see full spectra in **Figure S7**). The peaks of the predicted fragments are indicated with an asterisk.

To confirm the epoxidation of 430F-F5, LC-MS was performed on the third epoxidation with the possible products in **Figure 15** as target compounds. The LC-MS spectra showed that the molecular weights of the predicted products were present in multiple peaks at different retention times. To differentiate the targeted compounds from the isomers, compound **15e** was identified in the LC-MS spectra by the fragmentation pattern. The LC-MS method targeted 472 as MS 2 and 427 and MS 3, which are the possible fragments of compound **15e** (**Table 5**). The peaks of the fragmented masses of compound **15e** were present in the MS 2 and 3 at 49.92-50.91 and 54.78-55.37 minutes (**Table 5, Figures 16 and 17**), which indicated the presence of

compound **15e**. Both MS spectra showed a peak at 471.35 m/z and another peak coupled with formic acid at 517.35 m/z. The fragments in the MS 3 spectra (**Figures 16 and 17**) had different intensities at 327 m/z and 357 m/z. It is possible that the stereochemistry of compound **15e** at carbon 20 resulted in the different fragmentation, which affected its elution with five minutes apart. The fragmentation pattern of compound **15e** was not present in the LC-MS spectra of the natural 430F-F5, which confirmed that the formation of compound **15e** is likely from the result of the reaction. Since the fragmentation pattern for compound **15f** was not observed in the LC-MS spectra of the epoxidated 430F-F5, the reaction was more efficient in epoxidating the alkene on the alkyl chain than the cycloalkene. The presence of compound **15e** can be confirmed by isolating the compound using the preparative HPLC and elucidating the conformation of the structure with NMR. To detect the presence of other possible products in **Figure 15**, another LC-MS experiments can be performed with MS-MS and MS-MS-MS targeting different fragments.

The bioactivity of epoxidation 3 was assessed with the quorum sensing and growth inhibition assays. In the quorum quenching of *agr* III, the epoxidated 430F-F5 showed significant improvement between 4 and 64 $\mu\text{g/mL}$ (**Figure 18**). Unlike ammonolysis and bromination, epoxidation is predicted to modify the three-dimensional conformation of the triterpenoid skeleton. Epoxidation modifies the planar conformation of the alkene by introducing chiral centers. It is possible that the conformational change in the triterpenoid skeleton or the alkyl chain affected the inhibition of *agr* III.

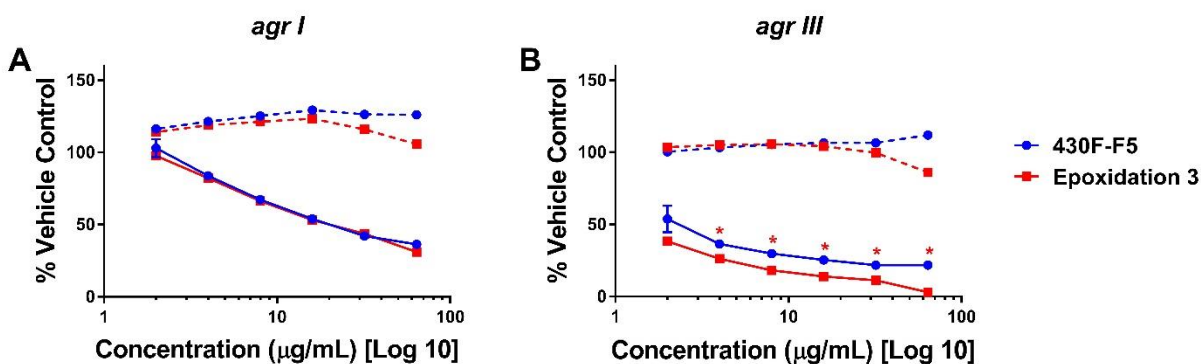


Figure 18: Epoxidation 3 shows decreased quorum quenching activity in (a) *agr I* and increased inhibition in (b) *agr III*. The solid lines represent the *agr* activity measured by fluorescence, and the dashed lines represent the growth of *S. aureus* measured by optical density. The asterisk indicates the significant difference of epoxidated 430F-F5 compared to natural 430F-F5 with P value less than 0.05 by multiple t-test.

Since epoxidation 3 showed the most improved quorum quenching activity among the modified 430F-F5, epoxidation 3 was separated into 40 fractions by using the preparative HPLC (**Figure 19**). The isolated compounds were also tested for quorum quenching activity and growth inhibition (**Figures 20** and **21**).

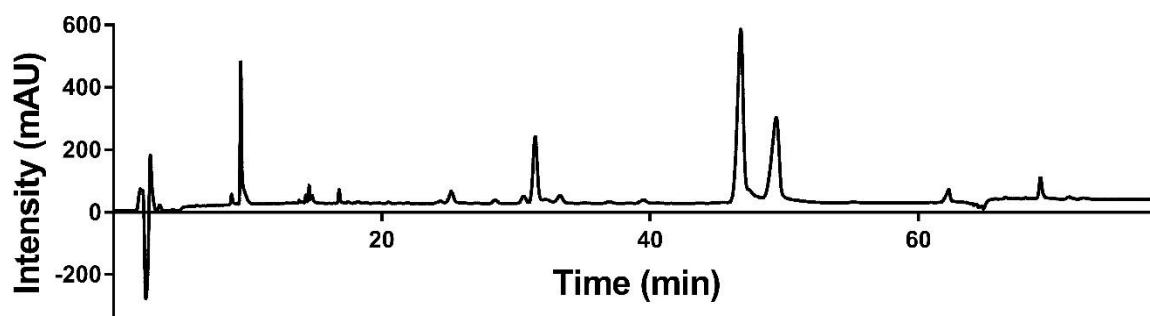


Figure 19: Preparative HPLC chromatograms of Epoxidation 3 at 217 nm.

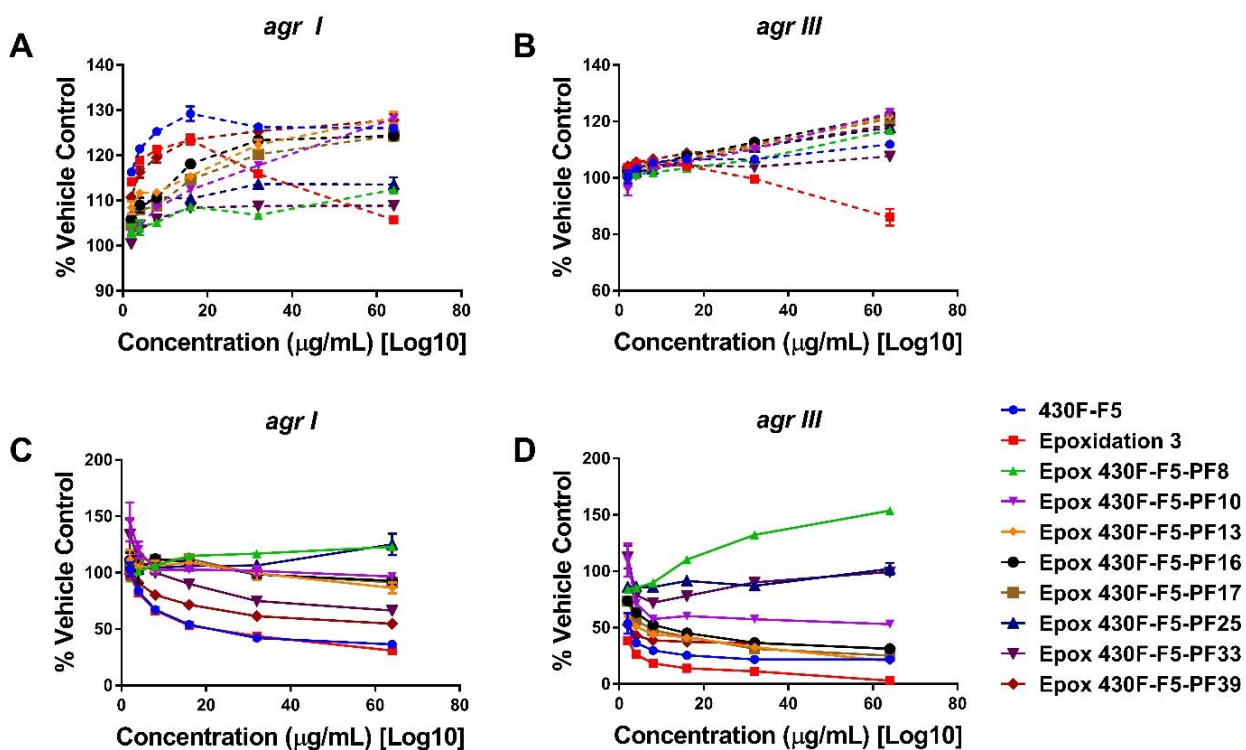


Figure 20: PF 8, 10, 13, 16, 17, 25, 33, and 39 from the epoxidated extract exhibit decreased quorum quenching activity in *agr I* and *III*. The dashed lines in A and B show the growth inhibition of *S. aureus*, and the solid lines in C and D represent quorum sensing inhibition in *S. aureus*.

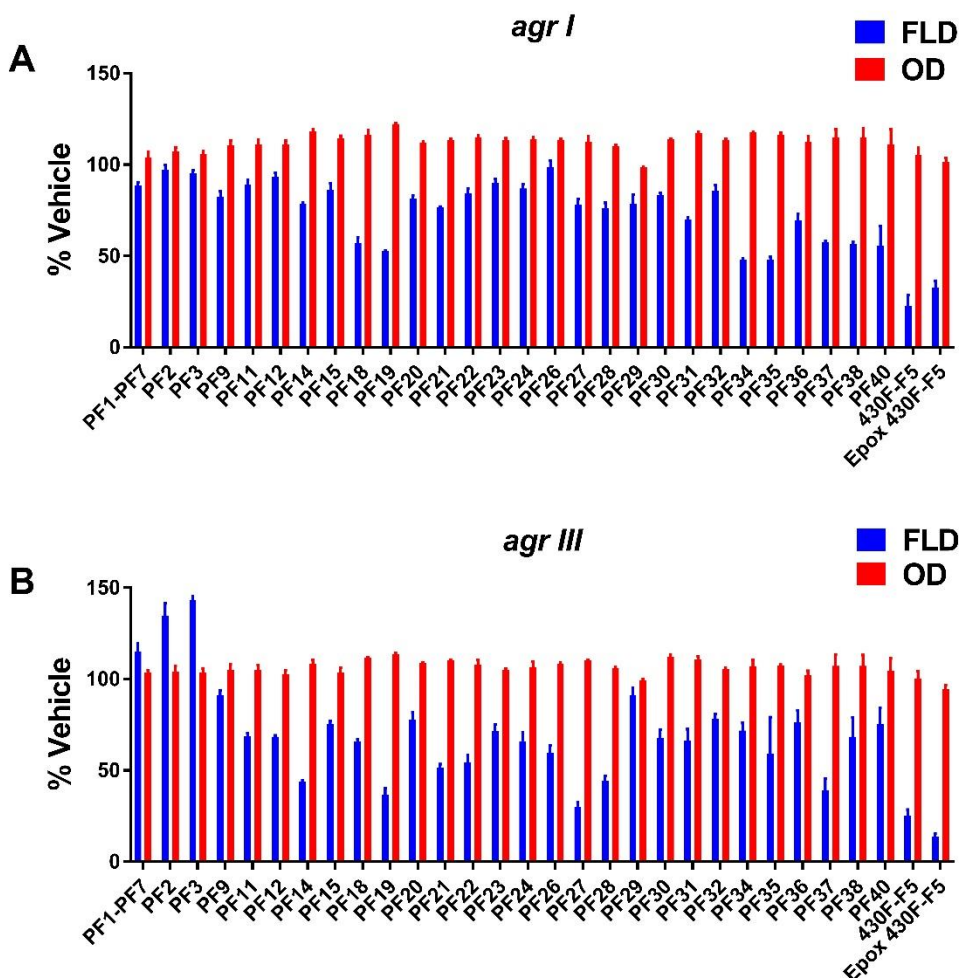


Figure 21: The partition fractions of epoxidated 430F-F5 show decreased quorum quenching activity at 32 $\mu\text{g}/\text{mL}$ in *agr I* and III. OD represent the optical density of *S. aureus* growth, and FLD represents the fluorescence from the expression of the *agr* gene.

Based on the high intensity of the peaks, the partition fractions 8, 10, 13, 16, 17, 25, 33 and 39 were tested for quorum quenching and growth inhibition against *agr I* and III from 2 to 64 $\mu\text{g}/\text{mL}$ (**Figure 20**). The remaining fractions were screened at a single concentration of 32 $\mu\text{g}/\text{mL}$ (**Figure 21**). The growth of *S. aureus* was not significantly inhibited by the fractions of epoxidated 430F-F5 (**Figures 20a, 20b and 21a**). While the epoxidated 430F-F5 increased the quorum quenching activity against *agr III* in **Figures 20d and 21b**, all fractions isolated from the

epoxidated 430F-F5 did not improve the quorum quenching activity in *agr* I and III compared to the natural 430F-F5. The decrease in quorum quenching activity can be explained by the degradation of compounds during the separation process using the preparative HPLC or the synergistic effect of the compounds.

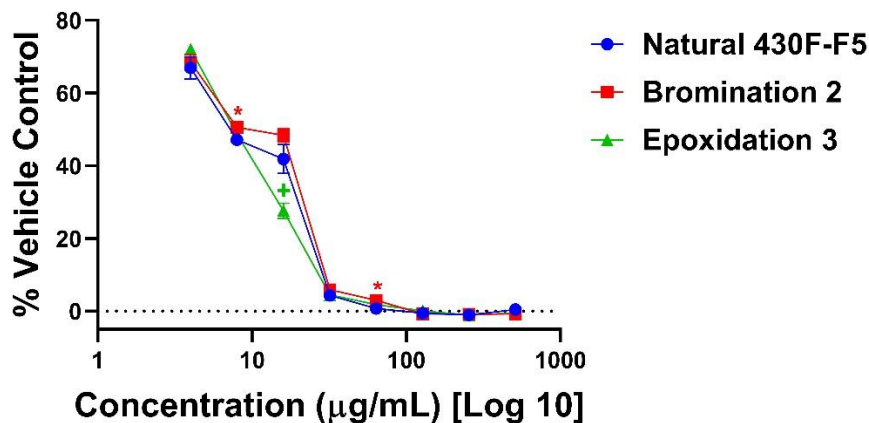


Figure 22: Cytotoxicity assay of natural 430F-F5, bromination 2 and epoxidation 3. Bromination 2 and epoxidation 3 show no significant change in cytotoxicity at most concentrations between 4 and 512 µg/mL. The asterisk (*) and plus sign (+) indicate the significant difference of brominated and epoxidated 430F-F5, respectively, compared to natural 430F-F5 with P value less than 0.05 by multiple t-test.

The cytotoxicity of the natural and modified extracts from bromination 2 and epoxidation 3 were also compared (**Figure 22**). The IC_{50} of the natural, brominated, and epoxidated 430F-F5 were 8 µg/mL. While the brominated 430F-F5 showed decreased cytotoxicity at 8 and 64 µg/mL, the cytotoxicity of epoxidated 430F-F5 increased at 16 µg/mL. At most concentrations between 4 and 512 µg/mL, the cytotoxicity of brominated and epoxidated 430F-F5 was not significantly different compared to the natural 430F-F5. The modification of the alkene did not significantly affect the cytotoxicity of the extract.

Since PF 27 exhibited the highest quorum quenching activity against *agr* III among the isolated fractions of epoxidation 3 (**Figure 22b**), ^1H NMR spectrum of PF 27 was obtained to check for the presence of an epoxide and elucidate the structure (**Figure 23**). While the NMR spectra of compound **1c** from the natural 430F-F5 and epoxidated 430F-F5-PF 27 were consisted of similar peaks in the alkyl region from 0.0 ppm to 2.5 ppm, the peaks of compound **1c** around 3.5 and 5.25 ppm have shifted to 4.0 ppm and 5.5 ppm, respectively. Further information such as ^{13}C NMR and MS spectra are needed to elucidate the structure of PF 27.

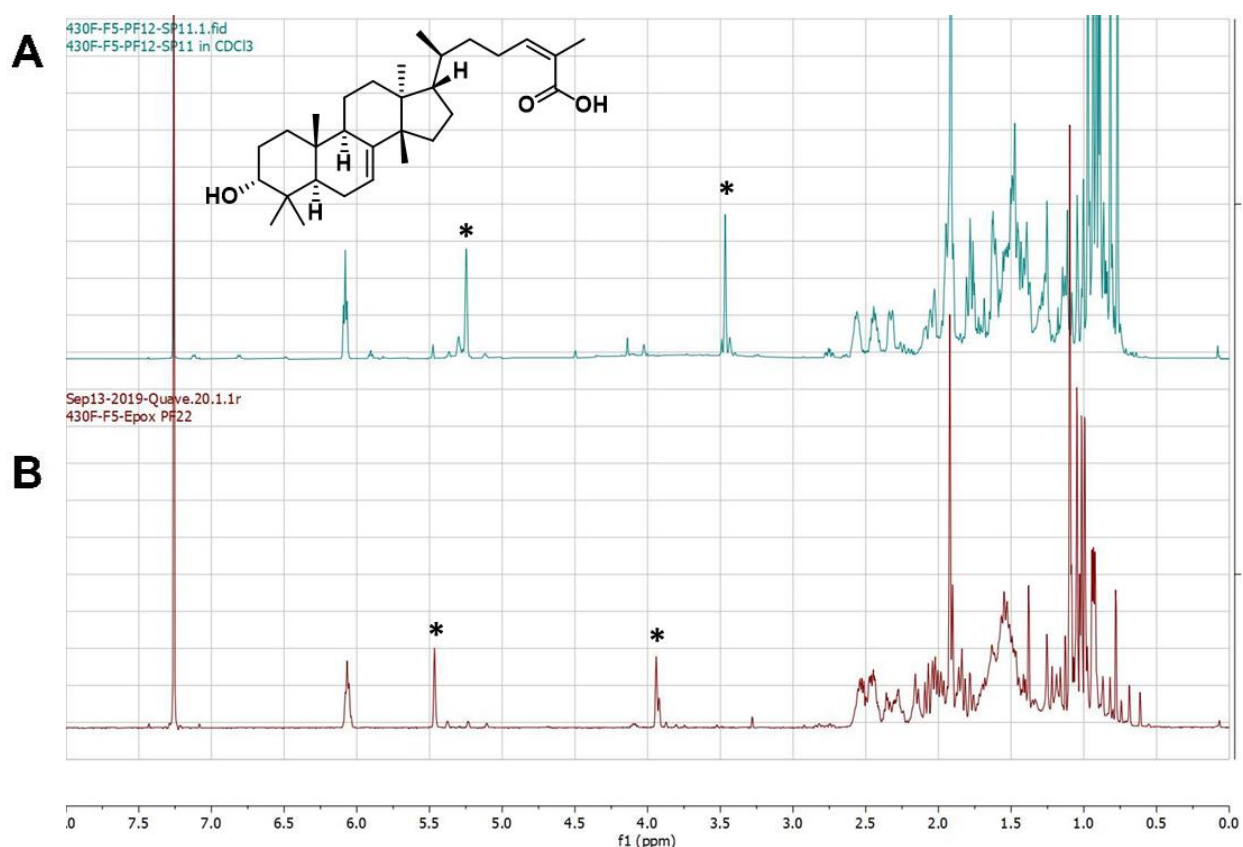


Figure 23: ^1H NMR spectra of a) triterpenoid from natural 430F-F5 and b) epoxidated 430F-F5-PF 27.

Chapter 5: Conclusion

In this study, the extract of *Schinus terebinthifolia* fruits modified by bromination and epoxidation showed improved quorum quenching activity against *agr* I and *agr* III in *S. aureus*, respectively, without increasing growth inhibition and cytotoxicity. After monitoring the process of the reactions by HPLC and NMR, the products of bromination and epoxidation were confirmed by using LC-MS with the triterpenoids from natural 430F-F5 (compounds **1a-c**) as precursors. The presence of the brominated products was verified with the 1:1 isotopic ratio in the LC-MS spectra. One of the epoxidated product was detected with the MS-MS and MS-MS-MS experiments targeting the fragments of the compound. To confirm the structures of the brominated and epoxidated triterpenoids, the compounds can be isolated with the preparative HPLC and elucidated by using NMR. While the ammonolyzed 430F-F5 decreased the quorum quenching activity, the brominated 430F-F5 slightly improved the inhibition of *agr* I, and the epoxidated 430F-F5 increased the inhibition of *agr* III. To optimize the quorum quenching activity of 430F-F5, other semisynthetic libraries can be generated from 430F-F5 using different reactions. The effect of the reactions on the bioactivity of plant extracts can be investigated by assessing the bioactivities of the modified 430F-F5 with different biological assays or testing the reactions on other plant extracts. The optimization of lead compounds with a quorum quenching activity can contribute to the drug development in treating MRSA infections.

References

1. CDC. Antibiotic Resistance Threats in the United States, 2013 2013. <https://www-cdc.gov.proxy.library.emory.edu/drugresistance/resources/publications.html>.
2. Wright, G. D.; Poinar, H., Antibiotic resistance is ancient: implications for drug discovery. *Trends in Microbiology* **2012**, *20* (4), 157-159.
3. Rossiter, S. E.; Fletcher, M. H.; Wuest, W. M., Natural products as platforms to overcome antibiotic resistance. *Chemical Reviews* **2017**, *117* (19), 12415-12474.
4. Muhs, A.; Lyles, J. T.; Parlet, C. P.; Nelson, K.; Kavanaugh, J. S.; Horswill, A. R.; Quave, C. L., Virulence inhibitors from Brazilian peppertree block quorum sensing and abate dermonecrosis in skin infection models. *Scientific Reports* **2017**, *7*, 42275.
5. Novick, R. P.; Geisinger, E., Quorum sensing in staphylococci. *Annual Review of Genetics* **2008**, *42*, 541-564.
6. Newman, D. J.; Cragg, G. M., Natural products as sources of new drugs from 1981 to 2014. *Journal of Natural Products* **2016**, *79* (3), 629-661.
7. Venugopal, A. A.; Johnson, S., Fidaxomicin: A Novel Macrocyclic Antibiotic Approved for Treatment of Clostridium difficile Infection. *Clinical Infectious Diseases* **2011**, *54* (4), 568-574.
8. Liu, R.; Li, X.; Lam, K. S., Combinatorial chemistry in drug discovery. *Current Opinion in Chemical Biology* **2017**, *38*, 117-126.
9. Nefzi, A.; Ostresh, J. M.; Yu, J.; Houghten, R. A., Combinatorial Chemistry: Libraries from Libraries, the Art of the Diversity-Oriented Transformation of Resin-Bound Peptides and Chiral Polyamides to Low Molecular Weight Acyclic and Heterocyclic Compounds. *The Journal of Organic Chemistry* **2004**, *69* (11), 3603-3609.
10. Méndez, L.; Salazar, M. O.; Ramallo, I. A.; Furlan, R. L., Brominated extracts as source of bioactive compounds. *ACS Combinatorial Science* **2010**, *13* (2), 200-204.
11. Ramallo, I. A.; Salazar, M. O.; Mendez, L.; Furlan, R. L. E., Chemically Engineered Extracts: Source of Bioactive Compounds. *Accounts of Chemical Research* **2011**, *44* (4), 241-250.
12. López, S. N.; Ramallo, I. A.; Sierra, M. G.; Zacchino, S. A.; Furlan, R. L., Chemically engineered extracts as an alternative source of bioactive natural product-like compounds. *Proceedings of the National Academy of Sciences* **2007**, *104* (2), 441-444.
13. Righi, D.; Marcourt, L.; Koval, A.; Ducret, V.; Pellissier, L.; Mainetti, A.; Katanaev, V. L.; Perron, K.; Wolfender, J.-L.; Queiroz, E. F., Chemo-diversification of plant extracts using a generic bromination reaction and monitoring by metabolite profiling. *ACS Combinatorial Science* **2019**, *21* (3), 171-182.
14. Tang, H.; Porras, G.; Brown, M. M.; Chassagne, F.; Lyles, J. T.; Bacsa, J.; Horswill, A. R.; Quave, C. L., Triterpenoid acid isolated from Schinus terebinthifolia fruits reduce Staphylococcus aureus virulence and abate dermonecrosis. *Scientific Reports* **2020** (In Review).
15. Chambers, H. F.; DeLeo, F. R., Waves of resistance: Staphylococcus aureus in the antibiotic era. *Nature Reviews Microbiology* **2009**, *7* (9), 629-641.
16. Dickey, S. W.; Cheung, G. Y. C.; Otto, M., Different drugs for bad bugs: antivirulence strategies in the age of antibiotic resistance. *Nature Reviews Drug Discovery* **2017**, *16* (7), 457-471.
17. Hua, L.; Hilliard, J. J.; Shi, Y.; Tkaczyk, C.; Cheng, L. I.; Yu, X.; Datta, V.; Ren, S.; Feng, H.; Zinsou, R.; Keller, A.; O'Day, T.; Du, Q.; Cheng, L.; Damschroder, M.; Robbie, G.; Suzich, J.; Stover, C. K.; Sellman, B. R., Assessment of an Anti-Alpha-Toxin Monoclonal

- Antibody for Prevention and Treatment of Staphylococcus aureus-Induced Pneumonia. **2014**, 58 (2), 1108-1117.
18. Zhang, J.; Liu, H.; Zhu, K.; Gong, S.; Dramsi, S.; Wang, Y.-T.; Li, J.; Chen, F.; Zhang, R.; Zhou, L.; Lan, L.; Jiang, H.; Schneewind, O.; Luo, C.; Yang, C.-G., Antiinfective therapy with a small molecule inhibitor of Staphylococcus aureus sortase. *PNAS* **2014**, 111 (37), 13517-13522.
 19. Boswihi, S. S.; Udo, E. E., Methicillin-resistant Staphylococcus aureus: An update on the epidemiology, treatment options and infection control. *Current Medicine Research and Practice* **2018**, 8 (1), 18-24.
 20. Ferry, T.; Perpoint, T.; Vandenesch, F.; Etienne, J., Virulence determinants in Staphylococcus aureus and their involvement in clinical syndromes. *Current Infectious Disease Reports* **2005**, 7 (6), 420.
 21. Cheraghi, S.; Pourgholi, L.; Shafaati, M.; Fesharaki, S. H.; Jalali, A.; Nosrati, R.; Boroumand, M. A., Analysis of virulence genes and accessory gene regulator (agr) types among methicillin-resistant Staphylococcus aureus strains in Iran. *Journal of Global Antimicrobial Resistance* **2017**, 10, 315-320.
 22. Khoramrooz, S. S.; Mansouri, F.; Marashifard, M.; Malek Hosseini, S. A. A.; Akbarian Chenarestane-Olia, F.; Ganavehei, B.; Gharibpour, F.; Shahbazi, A.; Mirzaii, M.; Darban-Sarokhalil, D., Detection of biofilm related genes, classical enterotoxin genes and agr typing among Staphylococcus aureus isolated from bovine with subclinical mastitis in southwest of Iran. *Microbial Pathogenesis* **2016**, 97, 45-51.
 23. Ikonomidis, A.; Vasdeki, A.; Kristo, I.; Maniatis, A. N.; Tsakris, A.; Malizos, K. N.; Pournaras, S., Association of biofilm formation and methicillin-resistance with accessory gene regulator (agr) loci in Greek Staphylococcus aureus clones. *Microbial Pathogenesis* **2009**, 47 (6), 341-344.
 24. Tu, Y., The discovery of artemisinin (qinghaosu) and gifts from Chinese medicine. *Nature Medicine* **2011**, 17 (10), 1217-1220.
 25. Panetta, F.; McKee, J., Recruitment of the invasive ornamental, Schinus terebinthifolius, is dependent upon frugivores. *Australian Journal of Ecology* **1997**, 22 (4), 432-438.
 26. Morton, J. F., Brazilian pepper—Its impact on people, animals and the environment. *Econ Bot* **1978**, 32 (4), 353-359.
 27. Fedel-Miyasato, L. E.; Formagio, A. S.; Auharek, S. A.; Kassuya, C. A.; Navarro, A. L.; Cunha-Laura, A. C.; Monreal, M. C.; Oliveira, R. J., Antigenotoxic and antimutagenic effects of Schinus terebinthifolius Raddi in Allium cepa and Swiss mice: a comparative study. *Genetics and Molecular Research* **2014**, 13 (2), 3411-3425.
 28. Piso, W.; Laet, J. d.; Marggraf, G.; Hackius, F.; Lud, E., *Historia naturalis Brasiliae ... :in qua non tantum plantae et animalia, sed et indigenarum morbi, ingenia et mores describuntur et iconibus supra quingentas illustrantur*. Apud Franciscum Hackium ;||Apud Lud. Elzevirium: Lugdun. Batavorum :||et Amstelodami :, 1648.
 29. Cseke, L. J.; Kirakosyan, A.; Kaufman, P. B.; Warber, S.; Duke, J. A.; Brielmann, H. L., *Natural products from plants*. CRC press: 2016.
 30. Moura-Costa, G. F.; Nocchi, S. R.; Ceole, L. F.; Mello, J. C. P. d.; Nakamura, C. V.; Dias Filho, B. P.; Temponi, L. G.; Ueda-Nakamura, T., Antimicrobial activity of plants used as medicinals on an indigenous reserve in Rio das Cobras, Paraná, Brazil. *Journal of Ethnopharmacology* **2012**, 143 (2), 631-638.

31. Nocchi, S. R.; Companhoni, M. V. P.; Mello, J. C. P. d.; Filho, B. P. D.; Nakamura, C. V.; Carollo, C. A.; Silva, D. B.; Ueda-Nakamura, T., Antiviral Activity of Crude Hydroethanolic Extract from *Schinus terebinthifolia* against Herpes simplex Virus Type 1. *Planta Med* **2017**, *234* (06), 509-518.
32. de Brito Marques Ramos, D.; de Moura Fontes Araújo, M. T.; de Lima Araújo, T. C.; dos Santos Neto, O. G.; e Silva, M. G.; Silva, Y. A.; Lira Torres, D. J.; de Siqueira Patriota, L. L.; de Melo, C. M. L.; de Lorena, V. M. B.; Guedes Paiva, P. M.; Mendes, R. L.; Napoleão, T. H., Evaluation of antitumor activity and toxicity of *Schinus terebinthifolia* leaf extract and lectin (SteLL) in sarcoma 180-bearing mice. *Journal of Ethnopharmacology* **2019**, *233*, 148-157.
33. Pichersky, E.; Noel, J. P.; Dudareva, N., Biosynthesis of plant volatiles: nature's diversity and ingenuity. *Science* **2006**, *311* (5762), 808-811.
34. Verhoff, M.; Seitz, S.; Paul, M.; Noha, S. M.; Jauch, J.; Schuster, D.; Werz, O., Tetra- and Pentacyclic Triterpene Acids from the Ancient Anti-inflammatory Remedy Frankincense as Inhibitors of Microsomal Prostaglandin E2 Synthase-1. *Journal of Natural Products* **2014**, *77* (6), 1445-1451.
35. Ku, J. M.; Hong, S. H.; Kim, H. I.; Lim, Y. S.; Lee, S. J.; Kim, M.; Seo, H. S.; Shin, Y. C.; Ko, S.-G., Cucurbitacin D exhibits its anti-cancer effect in human breast cancer cells by inhibiting Stat3 and Akt signaling. *European Journal of Inflammation* **2018**, *16*, 1721727X17751809.
36. Chen, J.; Li, W.; Yao, H.; Xu, J., Insights into drug discovery from natural products through structural modification. *Fitoterapia* **2015**, *103*, 231-241.
37. Dorwald, F. Z., *Lead Optimization for Medicinal Chemists: Pharmacokinetic Properties of Functional Groups and Organic Compounds*. Wiley-VCH Verlag GmbH & Co. KGaA: 2013.
38. Wunderlin, R. P.; Hansen, B. F., *Guide to the vascular plants of Florida*. University Press of Florida: 2003.
39. Roden, B. A.; El-Awa, A., Hydrazine. In *Encyclopedia of Reagents for Organic Synthesis*, American Cancer Society: 2014; pp 1-7.
40. Rao, A. S.; Mohan, H. R.; Iskra, J., Hydrogen Peroxide. In *Encyclopedia of Reagents for Organic Synthesis*, American Cancer Society: 2013.
41. Rao, A. S.; Mohan, H. R.; Charette, A., m-Chloroperbenzoic Acid. In *Encyclopedia of Reagents for Organic Synthesis*, American Cancer Society: 2005.
42. Caputo, M.; Lyles, J. T.; Salazar, M. S.; Quave, C. L., LEGO MINDSTORMS Fraction Collector: A Low-Cost Tool for a Preparative High-Performance Liquid Chromatography System. *Analytical Chemistry* **2020**, *92* (2), 1687-1690.
43. CLSI, *Performance standards for antimicrobial susceptibility testing: twenty-third informational supplement; M100-S23*. Clinical and Laboratory Standards Institute: 2013.
44. Quave, C. L.; Lyles, J. T.; Kavanaugh, J. S.; Nelson, K.; Parlet, C. P.; Crosby, H. A.; Heilmann, K. P.; Horswill, A. R., Castanea sativa (European Chestnut) Leaf Extracts Rich in Ursene and Oleanene Derivatives Block Staphylococcus aureus Virulence and Pathogenesis without Detectable Resistance. *PLOS ONE* **2015**, *10* (8), e0136486.
45. Bernini, R.; Pasqualetti, M.; Provenzano, G.; Tempesta, S., Ecofriendly synthesis of halogenated flavonoids and evaluation of their antifungal activity. *New Journal of Chemistry* **2015**, *39* (4), 2980-2987.
46. Llanos, G. G.; Araujo, L. M.; Jimenez, I. A.; Moujir, L. M.; Rodriguez, J.; Jimenez, C.; Bazzocchi, I. L., Structure-based design, synthesis, and biological evaluation of withaferin A-

analogues as potent apoptotic inducers. *European Journal of Medicinal Chemistry* **2017**, *140*, 52-64.

47. Sonego, J. M.; Cirigliano, A. M.; Cabrera, G. M.; Burton, G.; Veleiro, A. S. J. S., Synthesis and antifungal activity of C-21 steroids with an aromatic D ring. **2013**, *78* (7), 644-650.

48. Spectral Database for Organic Compounds (SDBS). National Institute of Advanced Industrial Science and Technology (AIST).

Supporting Information

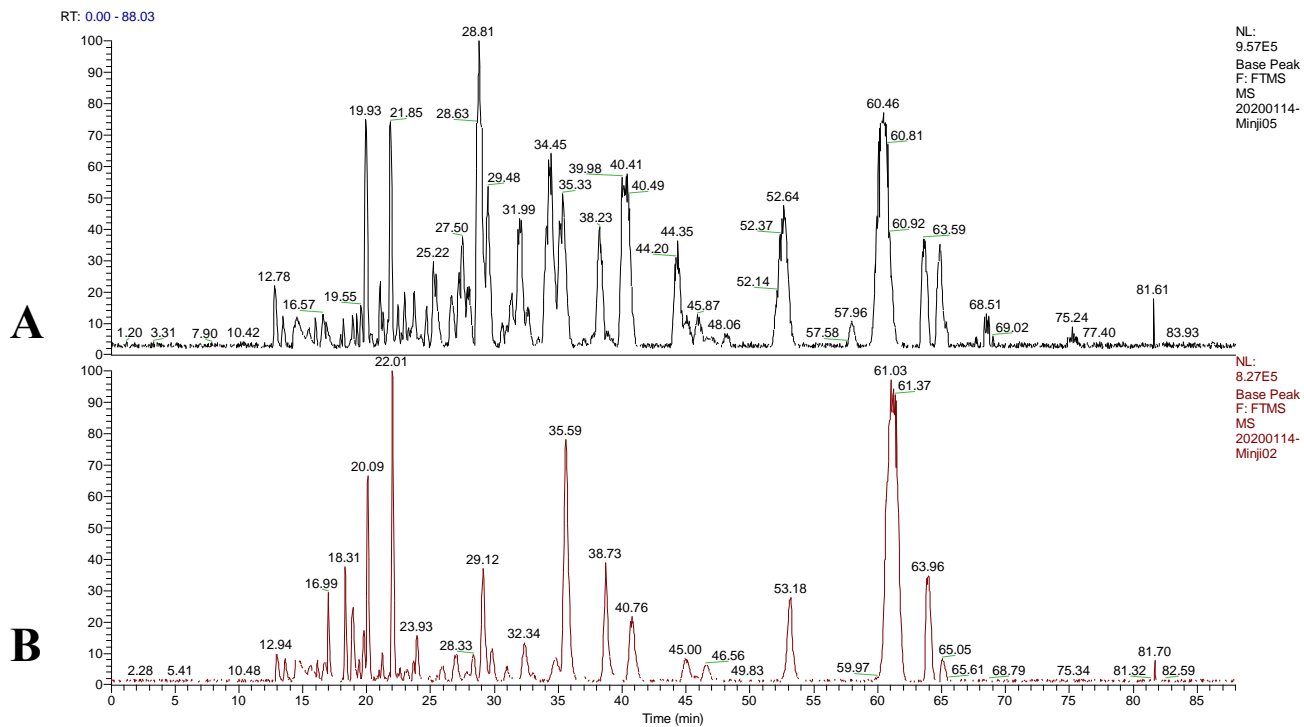
Figure S1: LC-MS chromatograms of brominated 430F-F5 in (a) positive mode and (b) negative mode.

Figure S2: MS spectra of $C_{30}H_{45}O_3Br$ in (a) positive mode at 63.12-64.11 minutes and (b) negative mode at 63.65-64.16 minutes from 150 to 1500 m/z.

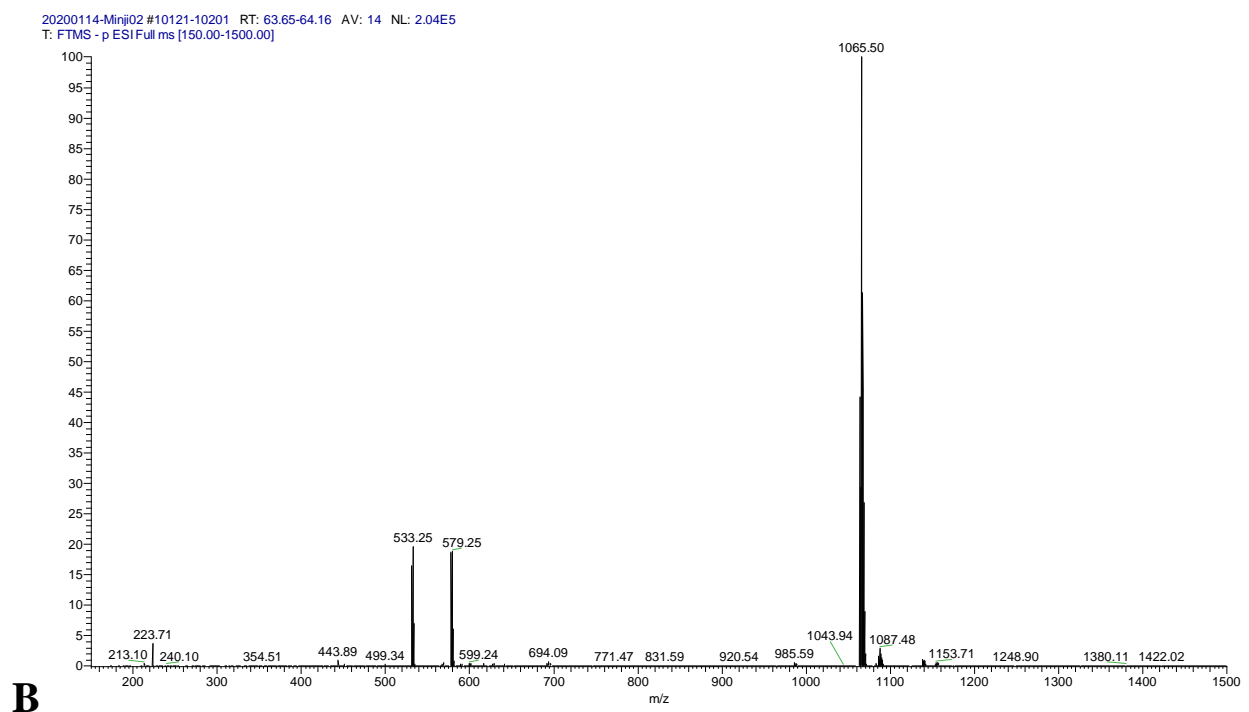
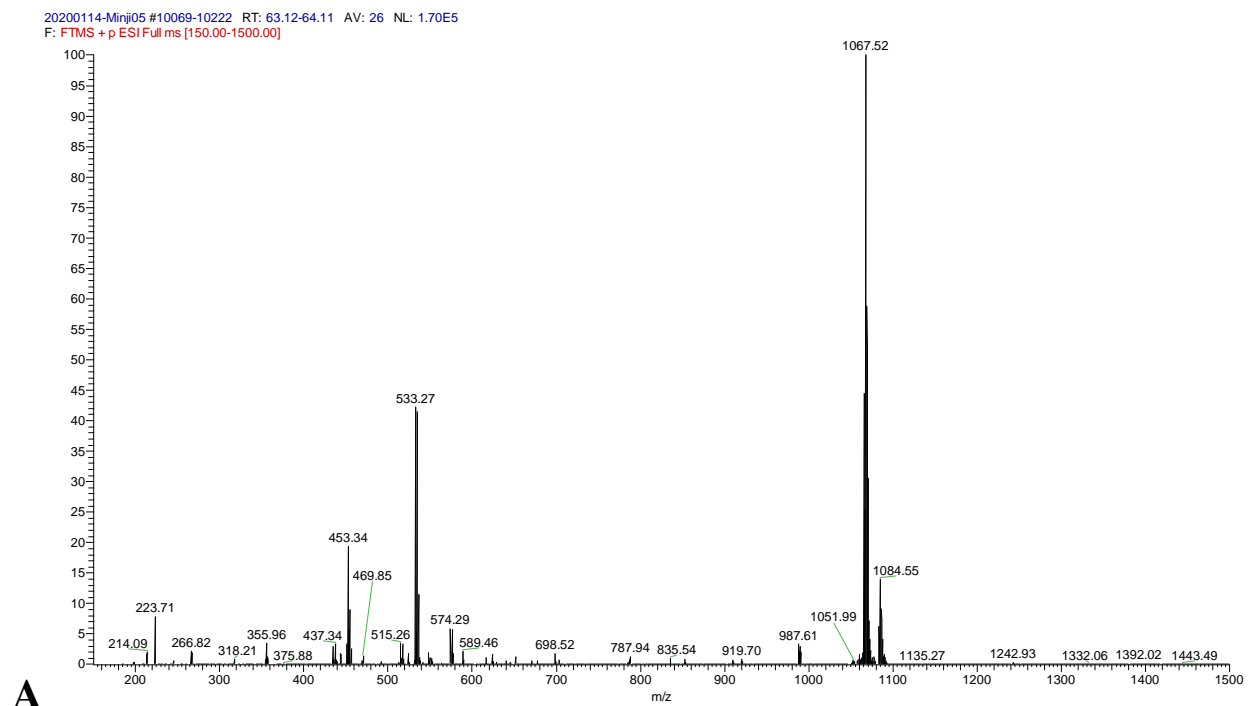


Figure S3: MS spectra of $C_{30}H_{47}O_3Br$ in (a) positive mode at 64.26-65.20 minutes and (b) negative mode at 52.84-53.79 minutes from 150 to 1500 m/z.

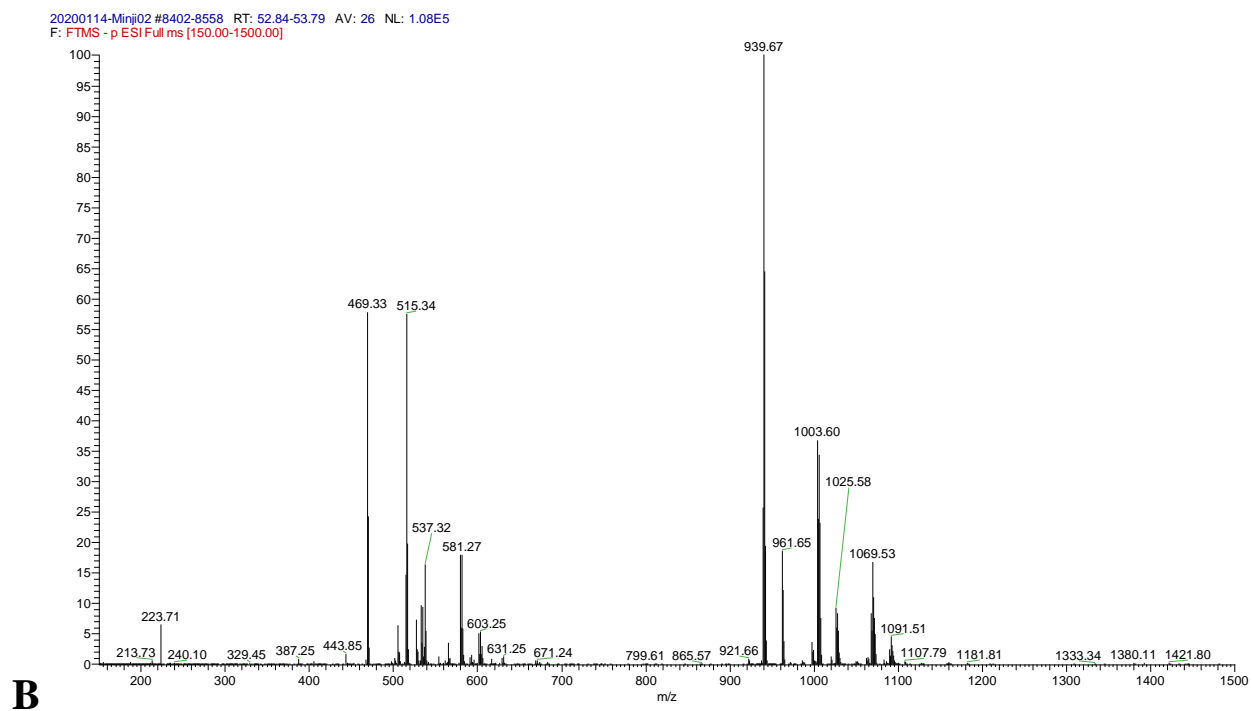
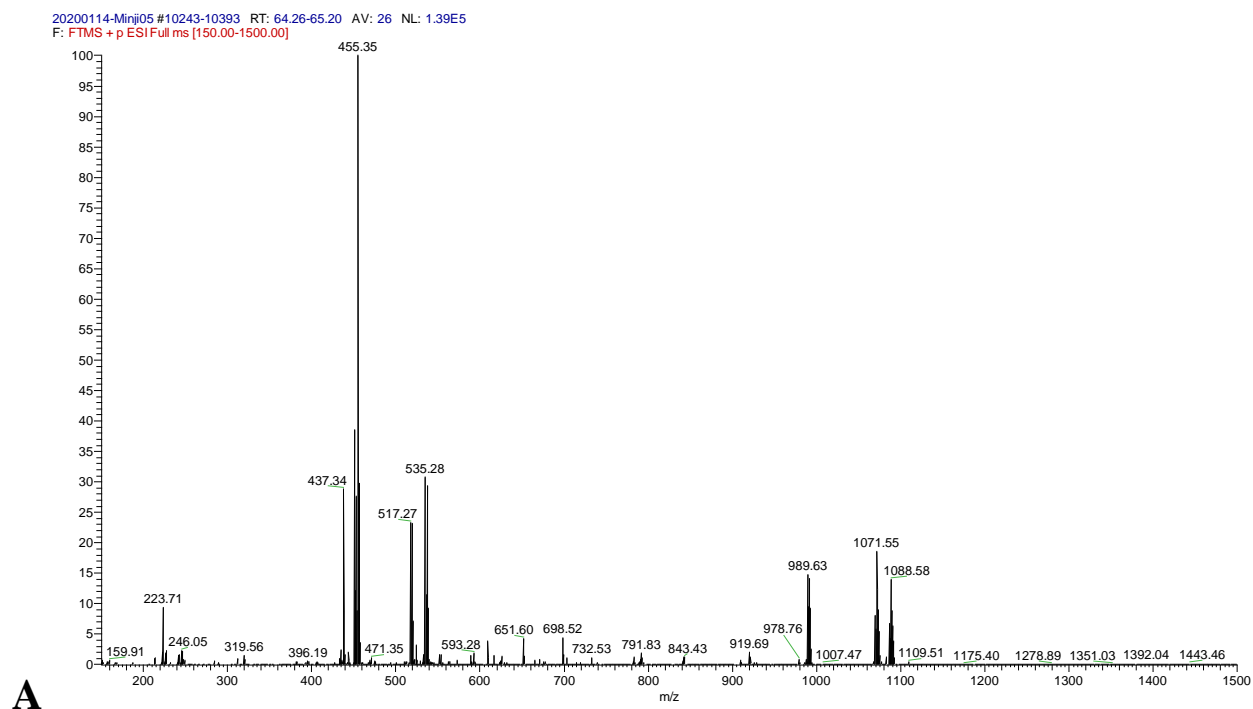
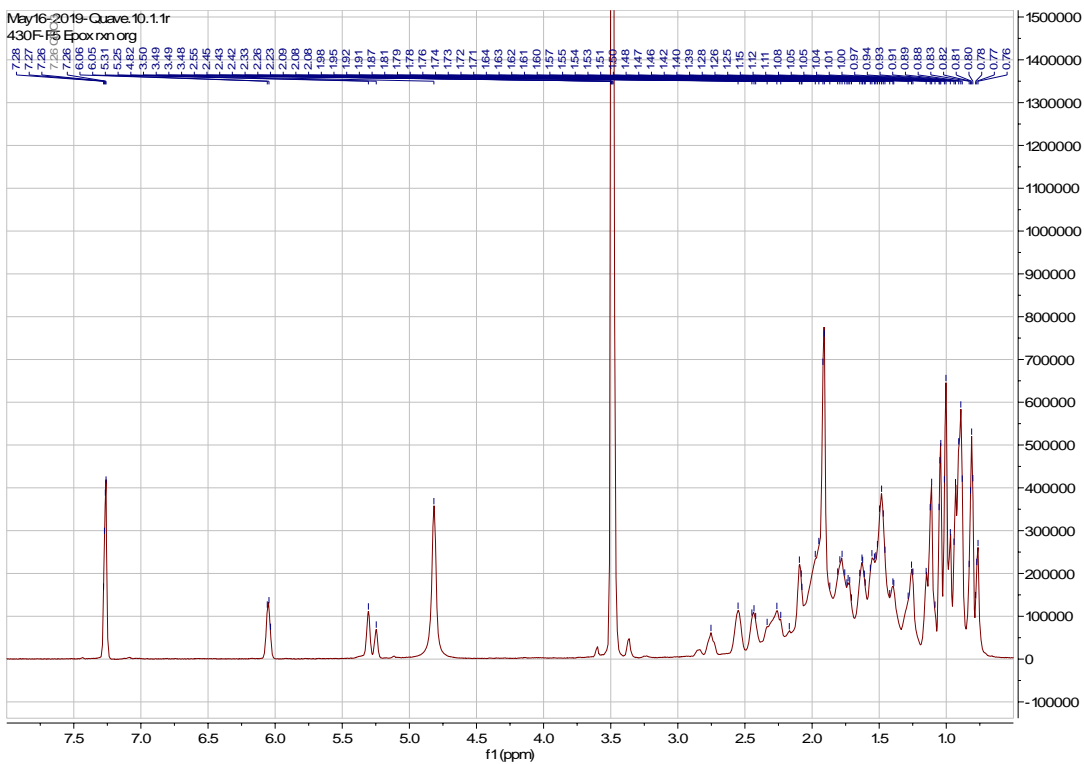
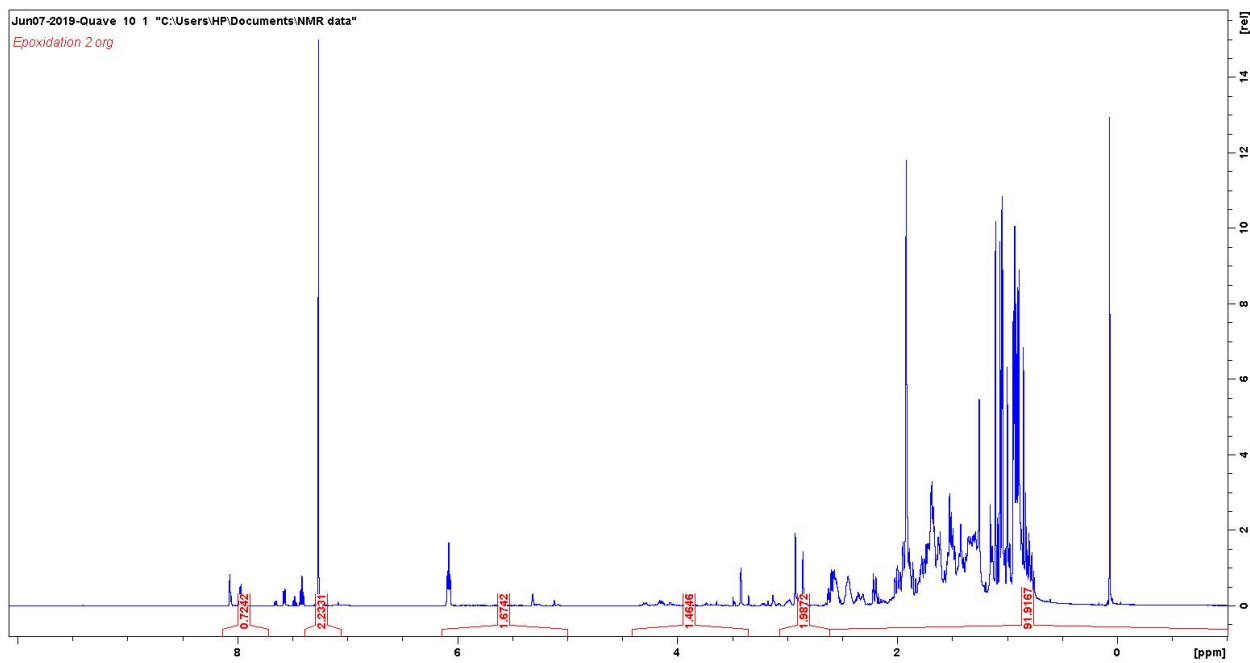


Figure S4: ^1H NMR spectra of epoxidation 1, 2, and 3 in CDCl_3 .

(a) Epoxidation 1



(b) Epoxidation 2



(c) Epoxidation 3

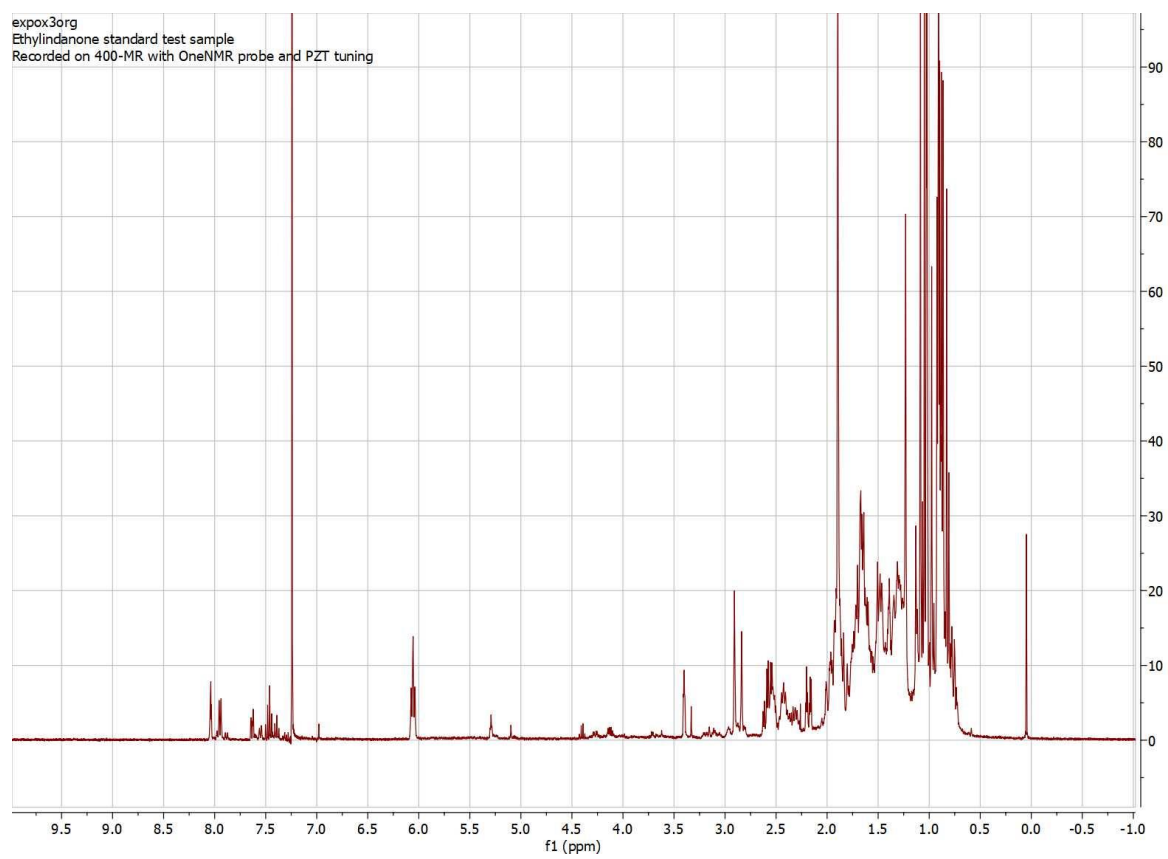


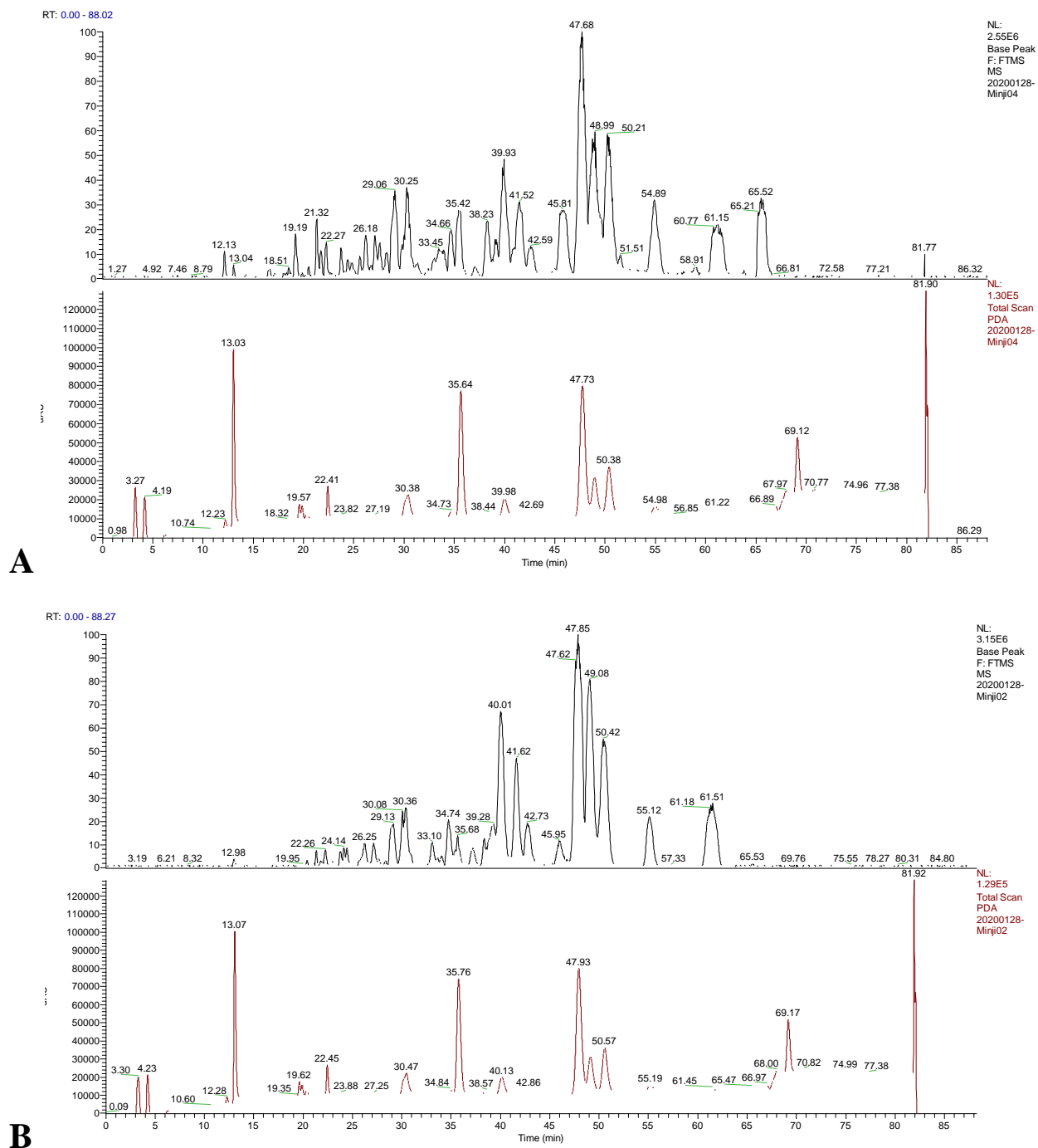
Figure S5: LC-MS chromatograms of epoxidated 430F-F5 in (a) positive and (b) negative mode.

Figure S6: MS spectra in negative mode for (a) MS of epoxidated 430F-F5, (b) MS 2 on 471 m/z, and (c) MS 3 on 427 m/z at 49.92-50.91 minutes from 150 to 1500 m/z.

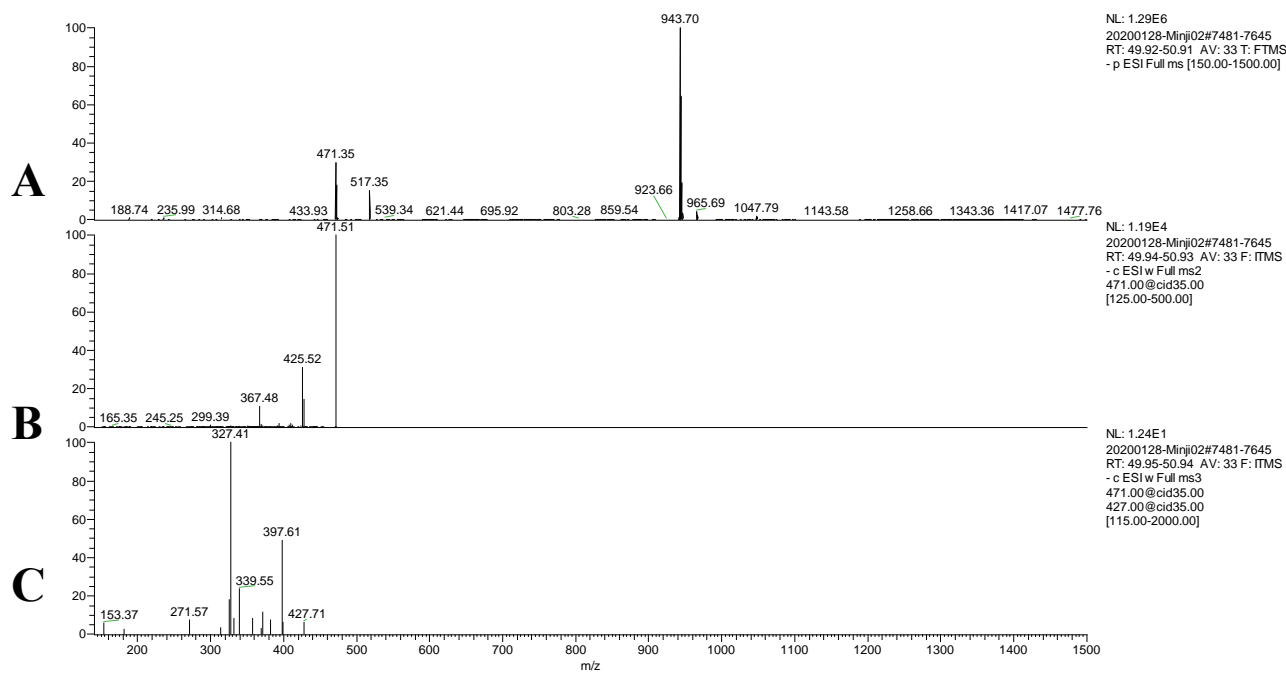


Figure S7: MS spectra in negative mode for (a) MS of epoxidated 430F-F5, (b) MS 2 on 471 m/z, and (c) MS 3 on 427 m/z at 54.78-55.37 minutes from 150 to 1500 m/z.

